

Response to the referees

Again, we thank Prof. Joel Savarino (the handling editor) and the anonymous reviewer for their time in reviewing our revised manuscript. Below, we give a point-by-point response to the comments and suggestions of the reviewers, in the order of (1) comments from Referees, (2) author's response, and (3) author's changes in manuscript (referee comments in black; [author's response and changes in manuscript in blue](#)).

The Reviewer #1

We thank the reviewer very much for his/her thoughtful review of our revised manuscript. All of the comments and suggestions have been taken into account, and are included in the revised version. Below, we give a point-by-point response to the comments and suggestions of the reviewer, in the order of (1) comments from Referees, (2) author's response, and (3) author's changes in manuscript (referee comments in black; author's response and changes in manuscript in blue).

(1) comments from Referees

The authors are to be commended for taking all reviewer comments seriously and implementing significant revisions to the manuscript. From my point of view I'd be happy to recommend publication after addressing the points below and carefully rechecking grammar/spelling:

(1) author's response

Again, we greatly appreciate the reviewer for his/her time in reviewing the revised version of the manuscript. We have carefully read the whole manuscript and improved grammar and spelling.

(1) author's changes in manuscript

Following the reviewer's comments, we carefully read the manuscript. Please see the revised version.

(2) comments from Referees

- please add to the introduction & discussion (4.2) the Halley study, something like:

Significant concentrations of organic nitrates (PAN and alkyl nitrates) were observed in the lower atmosphere at Halley in coastal Antarctica consistent with an oceanic source (Jones et al., 2011). They dominated the NO_y budget during the winter, and were on a par with inorganic nitrate compounds during the summer. Although not a direct source of snowpack nitrate, organic nitrates would act as a source of NO_x to coastal Antarctica that would ultimately contribute to nitrate within the snowpack (Jones et al., 2011). However, multi-seasonal measurements of surface snow nitrate correlate strongly with inorganic NO_y species (especially HNO₃) rather than organic (Jones et al., 2011).

(2) author's response

We thank the reviewer for the suggestion. The inorganic NO_3^- plays an important role in the atmospheric NO_y budget.

(2) author's changes in manuscript

Following the reviewer's suggestion, in the section of introduction, the statement was added, as follows,

At Halley station in coastal Antarctica, significant concentrations of organic nitrates (peroxyacetyl nitrate (PAN) and alkyl NO_3^-) were observed in the lower atmosphere (Jones et al., 2011). Organic nitrates dominated the NO_y (sum of reactive nitrogen oxide compounds) budget during the winter, and were on a par with inorganic nitrate compounds during the summer. Although not a direct source of snowpack NO_3^- , organic nitrates could act as source of NO_x to coastal Antarctica that would ultimately contribute to NO_3^- within the snowpack (Jones et al., 2011).

As the reviewer suggested, this point was also included in Discussion (4.2), as follows,

Although the organic nitrates can play an important role in the atmospheric NO_y budget, multi-seasonal measurements of surface snow NO_3^- correlate strongly with inorganic NO_y species (especially HNO_3) rather than organic (Jones et al., 2011).

For the changes, please see the revision-tracked version of manuscript, sections **1. Introduction, and 4.2 Effects of coexisting ions on NO_3^-**

(3) comments from Referees

- It is great that you include now the atmospheric observations. However, in my view they need to go into the main manuscript not just the supplementary material; e.g. add a panel to Fig.1 showing the variation with distance from the coast and make corresponding amendments to methods, results and discussion. Table S1 (move to main manuscript) must also include columns with site ID and sampling day.

As I pointed out before atmospheric NO_3^- is key to discuss and interpret an air-snow study of nitrate in snow. In fact, this is probably the only Antarctic traverse, which produced HiVol filter samples of atmospheric NO_3^- , very relevant to the entire discussion in this manuscript.

(3) author's response

We agree with the reviewer. The sampling and analysis methods of atmospheric NO_3^- were included in the section of methodology. The section of result and Figure 1 were revised accordingly. The full information about sampling location, sampling data, sample ID and chemical ion concentrations (NO_3^- and SO_4^{2-}) is present in Table S1 in supporting information.

(3) author's changes in manuscript

Following the reviewer's suggestion, the sampling method for atmospheric NO_3^- was included in section **2.2 Sample collection**, as follows,

To support understanding of the air-snow transfer of NO_3^- on the traverse, atmospheric NO_3^- was collected on glass fiber filters (Whatman G653) using a high volume air sampler (HVAS), with a flow rate of $\sim 1.0 \text{ m}^3 \text{ min}^{-1}$ for 12-15 hr, during the inland traverse campaign in 2015/2016. The NO_3^- collected on glass fiber filters are expected to equal the sum of particulate NO_3^- and gaseous HNO_3 , based upon previous investigations in East Antarctica (Savarino et al., 2007; Frey et al., 2009; Erbland et al., 2013). In total, 34 atmospheric samples were collected on the traverse. In addition, two field blanks were collected from filters installed in the HVAS without pumping and treated as samples thereafter. Detailed information about the atmospheric sampling is presented in Table S1 in supporting information.

After sample collection, all filters and snow samples were sealed in clean PE bags and preserved in clean thermal insulated boxes. All of the samples were transported to the laboratory under freezing conditions ($< -20 \text{ }^\circ\text{C}$).

Details on the analytical processing of atmospheric NO_3^- samples were added in **2.3 Sample analysis**, as follows,

In the laboratory, three quarters of individual filters were cut into pieces using pre-cleaned scissors that were rinsed between samples, placed in $\sim 100 \text{ ml}$ of Milli-Q water, ultrasonicated for 40 min and leached for 24 hr under shaking. The sample solutions were then filtered through $0.22 \text{ }\mu\text{m}$ ANPEL PTFE filters for NO_3^- concentration.

Accordingly, Figure 1 in the manuscript was revised, as follows, and the main results of the atmospheric NO_3^- investigation was included in section **3.1**.

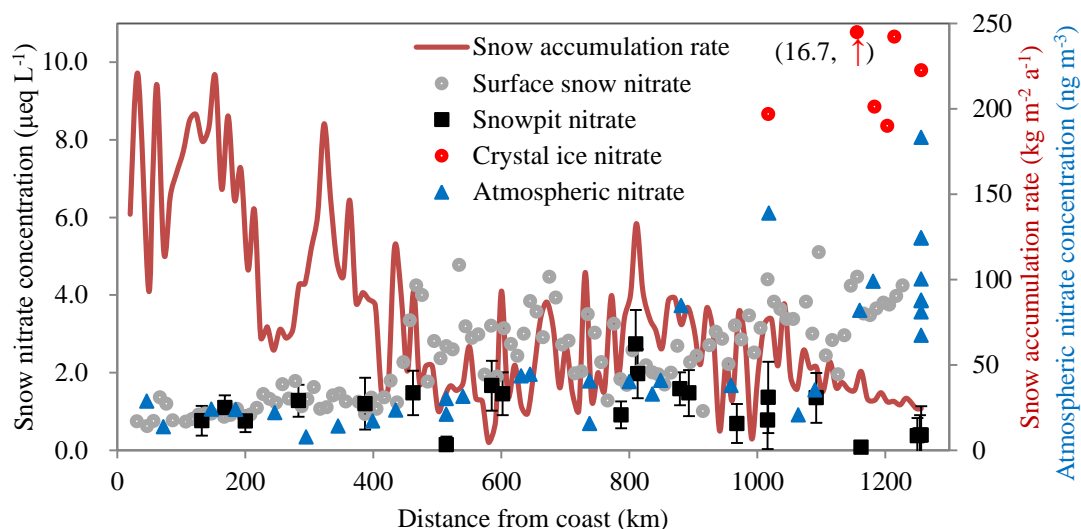


Figure 1. Concentrations of NO_3^- in snow (surface snow, crystal ice and snowpits; on the primary y-axis) and atmosphere (on the secondary y-axis), with error bars representing one standard deviation of NO_3^- (1σ) for individual snowpits. Also shown is the annual snow accumulation rate on the traverse (red solid line; based on Ding et al. (2011)). Note that NO_3^- concentration in one crystal ice sample (red dot), is higher than the maximum value of the primary y-axis (NO_3^- concentration = $16.7 \mu\text{eq L}^{-1}$ in the parentheses).

(4) comments from Referees

177-80 weird phrasing. Better: The late winter/early secondary maximum of nitrate observed in surface snow at coastal and inland locations has been attributed to the stratospheric source based on the nitrate stable isotopic composition (Legrand, 1989; Savarino, 2007; Frey, 2009).

(4) author's response

We thank the reviewer very much.

(4) author's changes in manuscript

Following the suggestion of the reviewer, the sentence was rephrased, as follows,

The late winter/early spring secondary maximum of NO_3^- observed in the atmosphere at coastal and inland locations has been attributed to the stratospheric source based on the NO_3^- stable isotopic composition (Legrand et al., 1989; Savarino et al., 2007; Frey et al., 2009).

(5) comments from Referees

184-90 I think you really need to distinguish between NO_3^- spikes and NO_3^- variability on decadal

to centennial or millennial time scales. A statistically significant link between the former and SPEs (solar proton events) has now been refuted. However, a link between the long-term variability of NO_3^- and solar cycles as suggested in Traversi et al. (2012) is very different in terms of time scales and likelihood of physical processes to be aligned, and may be present at some locations.

(5) author's response

We agree with the reviewer and thanks for the comment.

(5) author's changes in manuscript

Following the reviewer's comment, this paragraph was rephrased, as follows,

In addition, while some studies suggested that snow/ice NO_3^- is possibly linked with extraterrestrial fluxes of energetic particles and solar irradiation, with solar flares corresponding to NO_3^- spikes (Zeller et al., 1986; Smart et al., 2014), other observations and recent modeling studies have established that there is not a clear connection between solar variability and NO_3^- concentrations (Legrand et al., 1989; Legrand and Kirchner, 1990; Wolff et al., 2008; Wolff et al., 2012; Duderstadt et al., 2014; Duderstadt et al., 2016; Wolff et al., 2016). However, the potential link between the long-term (e.g., centennial to millennial time scales) variability of NO_3^- and solar cycles may be present at some locations (Traversi et al., 2012).

References

Duderstadt, K.A., Dibb, J.E., Jackman, C.H., Randall, C.E., Solomon, S.C., Mills, M.J., Schwadron, N.A., and Spence, H.E.: Nitrate deposition to surface snow at Summit, Greenland, following the 9 November 2000 solar proton event, *J. Geophys. Res.*, 119, 6938-6957, 2014.

Duderstadt, K.A., Dibb, J.E., Schwadron, N.A., Spence, H.E., Solomon, S.C., Yudin, V.A., Jackman, C.H., and Randall, C.E.: Nitrate ion spikes in ice cores not suitable as proxies for solar proton events, *J. Geophys. Res.*, 121, 2994-3016, doi:10.1002/2015JD023805, 2016.

Erbland, J., Vicars, W., Savarino, J., Morin, S., Frey, M., Frosini, D., Vince, E., and Martins, J.: Air-snow transfer of nitrate on the East Antarctic Plateau - Part 1: Isotopic evidence for a photolytically driven dynamic equilibrium in summer, *Atmos. Chem. Phys.*, 13, 6403-6419, doi:10.5194/acp-13-6403-2013, 2013.

Frey, M.M., Savarino, J., Morin, S., Erbland, J., and Martins, J.: Photolysis imprint in the nitrate stable isotope signal in snow and atmosphere of East Antarctica and implications for reactive nitrogen cycling, *Atmos. Chem. Phys.*, 9, 8681-8696, 2009.

Jones, A.E., Wolff, E.W., Ames, D., Bauguitte, S.-B., Clemmitshaw, K., Fleming, Z., Mills, G., Saiz-Lopez, A., Salmon, R.A., and Sturges, W.: The multi-seasonal NO_y budget in coastal Antarctica and its link with surface snow and ice core nitrate: results from the CHABLIS campaign, *Atmos. Chem. Phys.*, 11, 9271-9285, 2011.

Legrand, M., and Kirchner, S.: Origins and variations of nitrate in South Polar precipitation, *J. Geophys. Res.*, 95, 3493-3507 1990.

Legrand, M.R., Stordal, F., Isaksen, I.S.A., and Rognerud, B.: A model study of the stratospheric budget of odd nitrogen, including effects of solar cycle variations, *Tellus Series B-chemical & Physical Meteorology*, 41B, 413–426, doi:10.1111/j.1600- 0889.1989.tb00318.x, 1989.

Savarino, J., Kaiser, J., Morin, S., Sigman, D.M., and Thiemens, M.H.: Nitrogen and oxygen isotopic constraints on the origin of atmospheric nitrate in coastal Antarctica, *Atmos. Chem. Phys.*, 7, 1925-1945, 2007.

Smart, D.F., Shea, M.A., Melott, A.L., and Laird, C.M.: Low time resolution analysis of polar ice cores cannot detect impulsive nitrate events, *Journal of Geophysical Research: Space Physics*, 119, 9430-9440, doi:10.1002/2014JA020378, 2014.

Traversi, R., Usoskin, I., Solanki, S., Becagli, S., Frezzotti, M., Severi, M., Stenni, B., and Udisti, R.: Nitrate in Polar Ice: A New Tracer of Solar Variability, *Sol. Phys.*, 280, 237-254, 2012.

Wolff, E.W., Bigler, M., Curran, M., Dibb, J., Frey, M., Legrand, M., and McConnell, J.: The Carrington event not observed in most ice core nitrate records, *Geophys. Res. Lett.*, 39, L08503, doi:10.1029/2012GL051603, 2012.

Wolff, E.W., Bigler, M., Curran, M.A.J., Dibb, J.E., Frey, M.M., Legrand, M., and McConnell, J.R.: Comment on “Low time resolution analysis of polar ice cores cannot detect impulsive nitrate events” by D.F. Smart et al, *J. Geophys. Res.*, 121, 1920-1924, 2016.

Wolff, E.W., Jones, A.E., Bauguitte, S.-B., and Salmon, R.A.: The interpretation of spikes and trends in concentration of nitrate in polar ice cores, based on evidence from snow and atmospheric measurements, *Atmos. Chem. Phys.*, 8, 5627-5634, 2008.

Zeller, E.J., Dreschhoff, G.A., and Laird, C.M.: Nitrate flux on the Ross Ice Shelf, Antarctica and its relation to solar cosmic rays, *Geophys. Res. Lett.*, 13, 1264-1267, 1986.

End of the responses.

1 **Nitrate deposition and preservation in the snowpack along a traverse**
2 **from coast to the ice sheet summit (Dome A) in East Antarctica**

3
4 Guitao Shi^{1,2}, Meredith G. Hastings³, Jinhai Yu^{2,4}, Tianming Ma^{2,5}, Zhengyi Hu²,
5 Chunlei An², Chuanjin Li⁶, Hongmei Ma², Su Jiang², and Yuansheng Li²
6

7 ¹ Key Laboratory of Geographic Information Science (Ministry of Education) and School of
8 Geographic Sciences, East China Normal University, Shanghai 200241, China

9 ² Key Laboratory for Polar Science of State Oceanic Administration, Polar Research Institute of China,
10 Shanghai 200062, China

11 ³ Department of Earth, Environmental and Planetary Sciences and Institute at Brown for Environment
12 and Society, Brown University, Providence, Rhode Island 02912, USA.

13 ⁴ School of Geographic and Oceanographic Sciences, Nanjing University, Nanjing 210023, China

14 ⁵ School of Ocean and Earth Science, Tongji University, Shanghai 200092, China

15 ⁶ The State Key Laboratory of the Cryospheric Sciences, Northwest Institute of Eco-Environment and
16 Resources, Chinese Academy of Sciences, Lanzhou 730000, China

17
18 *Correspondence to:* G. Shi (gt_shi@163.com) and M.G. Hastings (meredith_hastings@brown.edu)
19
20
21

22 **Abstract.** Antarctic ice core nitrate (NO_3^-) can provide a unique record of the atmospheric reactive
23 nitrogen cycle. However, the factors influencing the deposition and preservation of NO_3^- at the ice sheet
24 surface must first be understood. Therefore, an intensive program of snow ~~sample collections~~and
25 ~~atmospheric sampling~~ was made on a traverse from the coast to the ice sheet summit, Dome A, East
26 Antarctica. Snow samples in this observation include 120 surface snow samples (top ~3 cm), 20
27 snowpits with depths of 150 to 300 cm, and 6 crystal ice samples (the topmost needle like layer on
28 Dome A plateau). The main purpose of this investigation is to characterize the distribution pattern and
29 preservation of NO_3^- concentrations in the snow in different environments. Results show that an
30 increasing trend of NO_3^- concentrations with distance inland is present in surface snow, and NO_3^- is
31 extremely enriched in the crystal ice (with a maximum of $16.1 \mu\text{eq L}^{-1}$). NO_3^- concentration profiles for
32 snowpits vary between coastal and inland sites. On the coast, the deposited NO_3^- was largely preserved,
33 and the archived NO_3^- fluxes are dominated by snow accumulation. The relationship between the
34 archived NO_3^- and snow accumulation rate can be well depicted by a linear model, suggesting a
35 homogeneity of atmospheric NO_3^- levels. It is estimated that dry deposition contributes 27-44 % of the
36 archived NO_3^- fluxes, and the dry deposition velocity and scavenging ratio for NO_3^- was relatively
37 constant near the coast. Compared to the coast, the inland snow shows a relatively weak correlation
38 between archived NO_3^- and snow accumulation, and the archived NO_3^- fluxes were more concentration
39 dependent. The relationship between NO_3^- and coexisting ions (nssSO_4^{2-} , Na^+ and Cl^-) was also
40 investigated, and the results show a correlation between nssSO_4^{2-} (fine aerosol particles) and NO_3^- in
41 surface snow, while the correlation between NO_3^- and Na^+ (mainly associated with coarse aerosol
42 particles) is not significant. In inland snow, there were no significant relationships found between NO_3^-
43 and the coexisting ions, suggesting a dominant role of NO_3^- recycling in determining the
44 concentrations.

45
46
47

1 Introduction

As the major sink of atmospheric nitrogen oxides ($\text{NO}_x = \text{NO}$ and NO_2), nitrate (NO_3^-) is one of the major chemical species measured in polar snow and ice. The measurements of NO_3^- in ice cores may offer potential for understanding the complex atmospheric nitrogen cycle as well as oxidative capacity of the atmosphere through time (Legrand and Mayewski, 1997; Alexander et al., 2004; Hastings et al., 2009; Geng et al., 2017). However, the sources, transported pathways, and preservation of NO_3^- in Antarctic snowpack are still not well understood in Antarctic snowpack, hampering the interpretation of ice core NO_3^- records.

The accumulation of NO_3^- in snow is associated with various environmental factors and continental, tropospheric and stratospheric sources could influence NO_3^- concentrations (Legrand and Kirchner, 1990; McCabe et al., 2007; Wolff et al., 2008; Lee et al., 2014). In surface snow, NO_3^- levels are thought to be linked with snow accumulation rate, and higher values are usually present in areas with low accumulation, e.g., East Antarctic plateaus (Qin et al., 1992; Erbland et al., 2013; Traversi et al., 2017). Unlike sea salt related ions (e.g., chloride (Cl^-), sodium (Na^+), and occasionally sulfate (SO_4^{2-})), NO_3^- does not usually show an elevated level in coastal Antarctic snow (Mulvaney and Wolff, 1994; Bertler et al., 2005; Frey et al., 2009), suggesting a negligible contribution from sea salt aerosols. However, the marine emissions of alkyl NO_3^- , particularly methyl and ethyl NO_3^- , produced in surface oceans by microbiological and/or photochemical processes, are thought to be a possible contribution to Antarctic NO_3^- (Jones et al., 1999; Liss et al., 2004). At Halley station in coastal Antarctica, significant concentrations of organic nitrates (peroxyacetyl nitrate (PAN) and alkyl NO_3^-) were observed in the lower atmosphere (Jones et al., 2011). Organic nitrates dominated the NO_y (sum of reactive nitrogen oxide compounds) budget during the winter, and were on par with inorganic nitrate compounds during the summer. Although not a direct source of snowpack nitrate, organic nitrates could act as source of NO_x to coastal Antarctica that would ultimately contribute to NO_3^- within the snowpack (Jones et al., 2011).

While industrial and/or agricultural emissions have contributed to increasing NO_3^- levels in Greenland snow and ice over recent decades to hundreds of years, the anthropogenic contribution to Antarctic NO_3^- is less clear (Mayewski and Legrand, 1990; Hastings et al., 2009; Felix and Elliott, 2013; Geng et al., 2014). Lightning and NO_x produced in the lower stratosphere have long been thought to play a major role (Legrand et al., 1989; Legrand and Kirchner, 1990). Recently, adjoint model simulations proposed that tropospheric transport of NO_3^- from mid-low latitude NO_x sources is an important source to the Antarctic year round, though less so in austral spring/summer (Lee et al., 2014). A recent treatment of NO_3^- in snow in the same global chemical transport model suggests that the recycling of NO_3^- and/or transport of NO_x due to photolysis of NO_3^- in the surface snow layer is important in determining summertime concentrations (Zatko et al., 2016). The stratospheric inputs of NO_3^- are thought to be the result of N_2O oxidation to NO , then formation of NO_3^- that is deposited via polar stratospheric cloud (PSC) sedimentation (Legrand et al., 1989; Legrand and Kirchner, 1990). The late winter/early spring secondary maximum of NO_3^- observed in the atmosphere at coastal and inland locations has been attributed to the stratospheric source based on the NO_3^- stable isotopic composition. This source has been used to explain sporadic NO_3^- concentration peaks and its associated isotopic composition in later winter and/or early spring at both coastal and inland locations (Legrand et al., 1989; Savarino et al., 2007; Frey et al., 2009). At some sites, the snow/ice core NO_3^- concentrations were found to be linked with regional atmospheric circulation (e.g., sea level pressure

92 gradient; Goodwin et al., 2003; Russell et al., 2006). In general, atmospheric circulation appears not to
93 affect snow NO_3^- concentrations directly, but indirectly through an influence on the air mass transport
94 and/or snow accumulation rate (Russell et al., 2004; Russell et al., 2006). In addition, while some
95 studies suggested that snow/ice NO_3^- is possibly linked with extraterrestrial fluxes of energetic particles
96 and solar irradiation, with solar flares corresponding to NO_3^- spikes (Zeller et al., 1986; Smart et al.,
97 2014), other observations and recent modeling studies have established that there is not a clear
98 connection between solar variability and NO_3^- concentrations (Legrand et al., 1989; Legrand and
99 Kirchner, 1990; Wolff et al., 2008; Wolff et al., 2012; Duderstadt et al., 2014; Duderstadt et al., 2016;
100 Wolff et al., 2016). However, the potential link between the long-term (e.g., centennial to millennial
101 time scales) variability of NO_3^- and solar cycles may be present at some locations (Traversi et al., 2012).
102 In summary, factors influencing NO_3^- levels in snow/ice are complicated, and the significance of the
103 relationship between NO_3^- and controlling factors varies temporally and spatially.

104 Gas phase and snow concentration studies, and recent isotopic investigations and modeling have
105 shown that NO_3^- , particularly in snow on the Antarctic plateau, is a combination of deposition of HNO_3
106 and post-depositional loss or recycling of NO_3^- (e.g., R thlisberger et al., 2002; Davis et al., 2004;
107 Dibb et al., 2004; Erbland et al., 2013; Erbland et al., 2015; Shi et al., 2015; Bock et al., 2016; Zatko
108 et al., 2016). Based upon a suite of isotopic studies in the field and laboratory, it has been demonstrated
109 that under cold, sunlit conditions ultraviolet photolysis dominates NO_3^- post-depositional processing,
110 whereas HNO_3 volatilization may become more important at warmer temperatures > -20 °C
111 (R thlisberger et al., 2002; Frey et al., 2009; Erbland et al., 2013; Berhanu et al., 2015). In snowpack,
112 the solar radiation decreases exponentially, with attenuation described in terms of an e -folding depth (z_e)
113 where the actinic flux is reduced to 37 % (i.e., $1/e$) of the surface value. Thus, about 95 % of snowpack
114 photochemistry is expected to occur above the depth of three times z_e (Warren et al., 2006). Field
115 measurements at Dome C on the East Antarctic plateau suggest a z_e of 10 to 20 cm (France et al., 2011),
116 and the depth is dependent upon the concentration of impurities contained in the snow (Zatko et al.,
117 2013). In the inland regions with low snow accumulation rates, particularly on the East Antarctic
118 plateaus, photolysis has been shown to lead to significant post-depositional loss of NO_3^- , demonstrated
119 by significant enrichment in ^{15}N of snow NO_3^- (i.e., high $\delta^{15}\text{N}$) (Frey et al., 2009; Erbland et al., 2013;
120 Berhanu et al., 2015; Erbland et al., 2015; Shi et al., 2015), as well as a decrease in $\delta^{18}\text{O}$ and $\Delta^{17}\text{O}$ due
121 to reformation of NO_3^- in the condensed phase (Erbland et al., 2013; Shi et al., 2015 and references
122 therein). The transport and recycling of NO_x sourced from photolysis of snow NO_3^- in the summertime
123 has been invoked to model the distribution of snowpack NO_3^- across the Antarctic plateau (Zatko et al.,
124 2016). However, snow physical characteristics play a crucial role in NO_3^- deposition and preservation.
125 For instance, summertime concentrations in the surface skin layer of snow (the uppermost ~4 mm) can
126 be explained as the result of co-condensation of HNO_3 and water vapour, with little to no photolytic
127 loss in this microlayer (Bock et al., 2016). The combination of concentration and isotopic studies, along
128 with physical aspects of the snow, could lead to the reconstruction and interpretation of atmospheric
129 NO_3^- over time (e.g., Erbland et al., 2015; Bock et al., 2016), if there is detailed understanding of the
130 NO_3^- deposition and preservation in different environments in Antarctica.

131 The effects of volatilization of NO_3^- are uncertain, given that one field experiment suggests that this
132 process is an active player in NO_3^- loss (17 % (-30 °C) to 67 % (-10 °C) of NO_3^- lost after two weeks'
133 physical release experiments; Erbland et al., 2013), while other laboratory and field studies show that
134 volatilization plays a negligible role in NO_3^- loss (Berhanu et al., 2014; Berhanu et al., 2015). Further
135 investigations are needed to quantify the effects of volatilization for a better understanding of NO_3^-

136 | preservation in ~~the~~ snow/ice. Based on z_e , NO_3^- at deeper depths in Antarctic snow (e.g., > 100 cm),
137 | well beyond the snow photic zone, may be taken as the archived fraction. Thus, NO_3^- in deeper snow
138 | possibly provides an opportunity to investigate the archived fraction and potential influencing factors
139 | (e.g., snow accumulation rate). Given that an extensive array of ice core measurements is unavailable
140 | in most of Antarctica, the deeper snowpits (with depth > 100 cm) may offer a useful way to investigate
141 | the archived NO_3^- .

142 | In the atmosphere in Antarctica, particularly during spring and summer, NO_3^- is found to be mainly
143 | in the form of gas phase HNO_3 , with NO_3^- concentration several times higher in gas phase than in the
144 | particulate phase (Piel et al., 2006; Legrand et al., 2017b; Traversi et al., 2017). During ~~the~~
145 | post-depositional processes, the uptake of gaseous HNO_3 is thought to be important in NO_3^-
146 | concentrations in surface snow layers (Udisti et al., 2004; Traversi et al., 2014; Traversi et al., 2017).
147 | Due to the high concentration in summer, HNO_3 appears to play an important role in acidifying sea-salt
148 | particles, possibly accounting for the presence of NO_3^- in the particulate phase in summer (Jourdain and
149 | Legrand, 2002; Legrand et al., 2017b; Traversi et al., 2017). It is noted that the significant increase of
150 | NO_3^- during the cold periods (e.g., Last Glacial Maximum) could be associated with its attachment to
151 | dust aerosol, instead of ~~the formation of~~ gas phase HNO_3 (Legrand et al., 1999; Wolff et al., 2010).

152 | To date, investigations on spatial and temporal patterns of snow NO_3^- have been performed on
153 | several traverses in Antarctica (e.g., 1990 International Trans-Antarctica Expedition, and DDU to
154 | Dome C; Qin et al., 1992; Bertler et al., 2005; Frey et al., 2009; Erbland et al., 2013; Pasteris et al.,
155 | 2014), but these provide an uneven distribution of snow NO_3^- concentrations, ~~and leave~~ ~~leaving~~ large
156 | regions un-sampled (e.g., Lambert Glacier basin and Dome A plateau). Over the past few decades,
157 | while several glaciological observations have been carried out on the Chinese inland Antarctic traverse
158 | route from Zhongshan to Dome A, East Antarctica (Hou et al., 2007; Ding et al., 2010; Ma et al., 2010;
159 | Ding et al., 2011; Li et al., 2013; Shi et al., 2015), the data on snow chemistry are still rare, particularly
160 | detailed information on NO_3^- . From 2009 to 2013, we therefore conducted surface snow and snowpit
161 | sampling campaigns along the traverse route, ~~and with~~ the main objectives ~~were to~~ (1) ~~to~~ describe NO_3^-
162 | distribution in surface snow and snowpits, (2) ~~to~~ characterize the relationship between archived NO_3^-
163 | and snow accumulation rate, and (3) ~~to~~ examine the potential effects of coexisting ions on NO_3^-
164 | preservation. The results of this study may help to better understand NO_3^- deposition and preservation
165 | in the snowpack, which is critical to the interpretation of ice core NO_3^- records.

166

167 | 2 Methodology

168

169 | 2.1 Study area (Zhongshan to Dome A traverse)

170 | The Zhongshan to Dome A CHINARE (Chinese National Antarctic Research Expedition) inland
171 | traverse is an important leg of the ITASE (International Trans-Antarctic Scientific Expedition). The
172 | traverse is in the Indian Ocean sector of East Antarctica, passing through the Lambert Glacier, the
173 | largest glacier in Antarctica. In January 1997 the first Chinese Antarctic inland expedition reached an
174 | area ~300 km from the coast; in January 1998 the traverse was extended to 464 km, and in December
175 | 1998, to the Dome A area ~1100 km from the coast. In the austral 2004/2005 summer for the first time,
176 | the traverse extended to the ice sheet summit, Dome A, a total distance of ~1260 km. In January 2009,
177 | the Chinese inland research base, Kunlun station (80°25'1.7"S and 77°6'58.0"E, 4087 m above mean
178 | sea level), was established at Dome A, mainly ~~aiming~~ ~~aimed~~ at deep ice core drilling and astronomical
179 | observations. Now, Kunlun base is a summer station, and the CHINARE team typically conducts an

180 annual inland traverse from the coastal Zhongshan station to Dome A.

181 In January 2010, the Dome A deep ice core project was started, and the construction of basic
182 infrastructure (including drill trench and scientific workroom) took 4 summer seasons. The deep ice
183 core drilling began in January 2013, and in total 801 m ice core was recovered by [the 2016/2017](#) season.
184 The investigation of NO_3^- deposition and preservation in the snowpack will be of help to the
185 interpretation of Dome A deep ice core NO_3^- records.

186

187 2.2 Sample collection

188 During the 2010/2011 CHINARE, surface snow samples (the topmost ~3 cm) were collected at an
189 interval of ~10 km along the traverse route from Zhongshan to Dome A, using 3.0 cm diameter
190 high-density polyethylene (HDPE) bottles (volume = 100 ml). The bottles were pre-cleaned with
191 Milli-Q ultrapure water (18.2 M Ω), until electrical conductivity of the water stored in bottles (> 24 h)
192 decreased to <0.5 $\mu\text{S cm}^{-1}$. Then, the bottles were dried under a class 100 super clean hood at 20 °C.
193 Immediately after the drying procedure, the bottles were sealed in clean PE bags that were not opened
194 until the field sampling started. At each sampling site (typically > 500 m away from the traverse route),
195 the bottles were pushed into surface snow layers in the windward direction. In total, 120 surface snow
196 samples were collected. In addition, at each sampling site, the upper snow density (~10 cm) was
197 measured using a density scoop with ~~the a~~ volume of 1000 cm^3 . ~~As the field blanks, p~~Pre-cleaned
198 bottles filled with Milli-Q water ~~were~~ taken to the field and treated to the same conditions as field
199 samples ~~to represent field blanks~~ ($n = 3$).

200 On the Dome A plateau, the snow is soft and non-cohesive, and morphology of the surface snow is
201 different from other areas on the traverse, with a needle ice crystal layer extensively developed, in
202 particular on the sastrugi (Fig. S1 in supporting information). The depth of the needle-like crystal ice
203 layer (referred to as ~~the~~ “crystal ice” in the following context) is generally < 1.0 cm. In order to
204 investigate air-snow transfer of NO_3^- in this uppermost ~1 cm layer, the crystal ice was collected using
205 a clean HDPE scoop, and then ~~was~~ poured into ~~the~~ clean wide mouth HDPE bottles. Approximately 30
206 g of crystal ice was collected for each sample. In total, 6 crystal ice samples were collected on the
207 traverse near Dome A plateau.

208 In addition to surface snow, snowpit samples were collected during CHINARE inland traverse
209 campaigns in 2009/2010, 2010/2011, and 2012/2013. The snowpits were excavated manually, and the
210 snow wall in the windward direction was scraped clean and flat with a clean HDPE scraper. Then the
211 bottles were pushed horizontally into the snow wall. Snowpit samples were collected from the base
212 towards the top layer along a vertical line. During the sampling process, all personnel wore PE gloves
213 and facemasks to minimize potential contamination. Note that the snowpits are generally > 1 km from
214 the traverse route to avoid possible contamination from the expedition activities. The full information
215 about individual snowpits, including location, distance from the coast, elevation, snowpit depth,
216 sampling resolution, collection date, and annual snow accumulation rate, is summarized in Table 1. All
217 together, 20 snowpits (SP1 to SP20 in Fig. 2, with SP20 corresponding to the location of Kunlun
218 station at Dome A) ~~as~~ 1741 snow samples, were collected.

219 To support understanding of the air-snow transfer of NO_3^- on the traverse, atmospheric NO_3^- was
220 collected on glass fiber filters (Whatman G653) using a high volume air sampler (HVAS), with a flow
221 rate of ~1.0 $\text{m}^3 \text{min}^{-1}$ for 12-15 hr, during the inland traverse campaign in 2015/2016. The NO_3^-
222 collected on glass fiber filters are expected to equal the sum of particulate NO_3^- and gaseous HNO_3 ,
223 based upon previous investigations in East Antarctica (Savarino et al., 2007; Frey et al., 2009; Erbland

224 [et al., 2013](#)). In total, 34 atmospheric samples were collected on the traverse. In addition, two field
225 blanks were collected from filters installed in the HVAS without pumping and treated as samples
226 thereafter. Detailed information about the atmospheric sampling is presented in Table S1 in supporting
227 information.

228 After sample collection, all filters and snow samples ~~After snow collection, the bottles~~ were sealed in
229 clean PE bags ~~again~~ and preserved in clean thermal insulated boxes. All of the samples were
230 transported to the laboratory under freezing conditions (< -20 °C).

231

232 2.3 Sample analysis

233 In the laboratory, three quarters of individual filters were cut into pieces using pre-cleaned scissors
234 that were rinsed between samples, placed in ~100 ml of Milli-Q water, ultrasonicated for 40 min and
235 leached for 24 hr under shaking. The sample solutions were then filtered through 0.22 μm ANPEL
236 PTFE filters for concentration analysis. Snow samples were melted in the closed sampling bottles on a
237 super clean bench (class 100) before chemical measurements. Analyses of Na^+ , NH_4^+ , K^+ , Mg^{2+} , Ca^{2+} ,
238 Cl^- , NO_3^- and SO_4^{2-} were performed using a Dionex ICS-3000 ion chromatography system. The column
239 used for cation analysis (Na^+ , NH_4^+ , K^+ , Mg^{2+} and Ca^{2+}) was a Dionex column CS12 (2 \times 250 mm), with
240 a guard column CG12 (2 \times 50 mm); while the anions (Cl^- , NO_3^- and SO_4^{2-}) were analyzed using a
241 Dionex column AS11 (2 \times 250 mm) with a guard column AG11 (2 \times 50 mm). The eluent for cations was
242 18.0 mM methanesulfonic acid (MSA), and the gradient elution method was employed for anion
243 analysis, with eluent of potassium hydroxide (KOH). More details on this method are described in a
244 previous report (Shi et al., 2012). During sample analysis, duplicated samples and field blanks were

245 synchronously analyzed. The pooled standard deviation (σ_p , $\sigma_p = \sqrt{\sum_{i=1}^k (n_i - 1)s_i^2 / \sum_{i=1}^k (n_i - 1)}$,
246 where n_i and s_i^2 are the size and variance of the i th samples respectively, and k is the total number of
247 sample sets) of all replicate samples run at least twice in two different sample sets is 0.019 (Cl^-), 0.023
248 (NO_3^-), 0.037 (SO_4^{2-}), 0.022 (Na^+), 0.039 (NH_4^+), 0.006 (K^+), 0.006 (Mg^{2+}) and 0.006 (Ca^{2+}) $\mu\text{eq L}^{-1}$
249 respectively ($n = 65$ pairs of samples). Ion concentrations in field blanks ($n = 3$) are generally lower
250 than the detection limit (DL, 3 standard deviations of water blank in the laboratory).

251 For Antarctic snow samples, the concentrations of H^+ are usually not measured directly, but deduced
252 from the ion-balance disequilibrium in the snow. Here, H^+ concentration is calculated through ion
253 balance.

$$254 [\text{H}^+] = [\text{Cl}^-] + [\text{NO}_3^-] + [\text{SO}_4^{2-}] - [\text{Na}^+] - [\text{NH}_4^+] - [\text{Mg}^{2+}] - [\text{Ca}^{2+}] \text{ (Eq. 1),}$$

255 where ion concentrations are in $\mu\text{eq L}^{-1}$. In addition, the non-sea salt fractions of SO_4^{2-} (nssSO_4^{2-}) and
256 Cl^- (nssCl^-) can be calculated from the following expressions, by assuming Na^+ exclusively from sea
257 salt (in $\mu\text{eq L}^{-1}$).

$$258 [\text{nssSO}_4^{2-}] = [\text{SO}_4^{2-}] - 0.12 \times [\text{Na}^+] \text{ (Eq. 2),}$$

$$259 [\text{nssCl}^-] = [\text{Cl}^-] - 1.17 \times [\text{Na}^+] \text{ (Eq. 3).}$$

260 It is noted that SO_4^{2-} fractionation (the precipitation of mirabilite ($\text{Na}_2\text{SO}_4 \cdot 10\text{H}_2\text{O}$)) may introduce a
261 bias in nssSO_4^{2-} , particularly during the winter half year (Wagenbach et al., 1998a).

262

263 3 Results

264

265 3.1 NO_3^- concentration in surface snow

266 Concentrations of NO_3^- in surface snow are shown in Fig. 1, ranging from 0.6 to 5.1 $\mu\text{eq L}^{-1}$, with a

267 mean of $2.4 \mu\text{eq L}^{-1}$. One standard deviation (1σ) of NO_3^- concentration in surface snow is $1.1 \mu\text{eq L}^{-1}$,
268 with coefficient of variation (C_v , 1σ over mean) of 0.5, indicating a moderate spatial variability. On the
269 coastal ~ 450 km, NO_3^- shows a slightly increasing trend towards the interior, with a low variability,
270 while NO_3^- concentrations are higher in the inland region, with a large fluctuation. It is notable that in
271 the area ~ 800 km from the coast, where snow accumulation is relatively high, NO_3^- concentrations
272 decrease to $< 2.0 \mu\text{eq L}^{-1}$, comparable to the values on the coast. Near the Dome A plateau (> 1000 km
273 from coast), there is a tendency for higher NO_3^- concentrations ($> 5.0 \mu\text{eq L}^{-1}$). Similarly, atmospheric
274 NO_3^- concentrations increase from the coast towards the plateau, ranging from 8 to 183 ng m^{-3} (mean =
275 55 ng m^{-3}) (Fig. 1).

276 The percentage that surface snow NO_3^- contributes to total ions (i.e., total ionic strength, sum of Na^+ ,
277 NH_4^+ , K^+ , Mg^{2+} , Ca^{2+} , Cl^- , NO_3^- , SO_4^{2-} and H^+ , in $\mu\text{eq L}^{-1}$) varies from 6.7 to 37.6 % (mean = 27.0 %;
278 Fig. S2 in supporting information), with low values near the coast and high percentages on the plateau.
279 A strong relationship was found between NO_3^- and the total ionic strength in surface snow ($R^2 = 0.55$, p
280 < 0.01).

281 In the crystal ice, the means (ranges) of Cl^- , NO_3^- , SO_4^{2-} , Na^+ , NH_4^+ , K^+ , Mg^{2+} , Ca^{2+} and H^+
282 concentrations are 0.98 (0.62 – 1.27), 10.40 (8.35 – 16.06), 1.29 (0.87 – 2.13), 0.27 (0.21 – 0.33), 0.24
283 (0.03 – 0.56), 0.05 (0.03 – 0.08), 0.18 (0.15 – 0.22), 0.18 (0.05 – 0.57) and 11.75 ($9.56 - 18.12$) $\mu\text{eq L}^{-1}$,
284 respectively. H^+ and NO_3^- are the most abundant species, accounting for 46.4 and 41.0 % of the total
285 ions, followed by SO_4^{2-} (5.1 %) and Cl^- (3.9 %). The other 5 cations, Na^+ , NH_4^+ , K^+ , Mg^{2+} and Ca^{2+} ,
286 only represent 3.6 % of the total ion budget. A significant linear relationship was found between NO_3^-
287 and the total ionic strength ($R^2 = 0.99$, $p < 0.01$), possibly suggesting that NO_3^- is the species
288 controlling ion abundance by influencing acidity of the crystal ice (i.e., H^+ levels). In comparison with
289 surface snow, concentrations of H^+ and NO_3^- are significantly higher in crystal ice (Independent
290 Samples T Test, $p < 0.01$), while concentrations of Cl^- , SO_4^{2-} , Na^+ , NH_4^+ , K^+ , Mg^{2+} and Ca^{2+} are
291 comparable in the two types of snow samples (Fig. S2 in supporting information). To date, the
292 information on the chemistry of ice crystal is rather limited but data from the so-called skin layer at
293 Dome C (top ~ 4 mm snow), where NO_3^- concentrations are in the range of $9 - 22 \mu\text{eq L}^{-1}$ in
294 summertime (Erbland et al., 2013), are generally comparable to our observations.

295 NO_3^- concentrations in surface snow have been widely measured across Antarctica (Fig. 2), and the
296 values vary from 0.2 to $12.9 \mu\text{eq L}^{-1}$, with a mean of $2.1 \mu\text{eq L}^{-1}$ ($n = 594$, $1\sigma = 1.7 \mu\text{eq L}^{-1}$) and a
297 median of $1.4 \mu\text{eq L}^{-1}$. Most of the data (87 %) fall in the range of $0.5 - 4.0 \mu\text{eq L}^{-1}$, and only 7 % of the
298 values are above $5.0 \mu\text{eq L}^{-1}$, mainly distributed on the East Antarctic plateaus. Spatially, NO_3^-
299 concentrations show an increasing trend with distance inland, and the values are higher in East than in
300 West Antarctica. Overall, this spatial pattern is opposite to that of the annual snow accumulation rate
301 (Arthern et al., 2006), i.e., low (high) snow accumulation corresponds to high (low) NO_3^-
302 concentrations. It is difficult to compare with NO_3^- concentrations derived from the “upper snow layer”
303 in different studies because each study sampled a different depth (Fig. 2), e.g., 2 - 10 cm for
304 DDU-Dome C traverse (Frey et al., 2009; Erbland et al., 2013), 25 cm for the 1989-1990 International
305 Trans-Antarctica Expedition (Qin et al., 1992) and 3 cm for this study. The different sampling depths
306 can result in large differences in NO_3^- concentration, especially on the East Antarctic plateaus (e.g., the
307 values of the topmost 1 cm of snow, the crystal ice in this study, can be up to $>15 \mu\text{eq L}^{-1}$; Fig. 1). ~~In~~
308 ~~this case~~ Because of this, any comparison of NO_3^- concentrations in surface snow collected in different
309 campaigns should be made with caution.

310

311 3.2 Snowpit NO₃⁻ concentrations

312 Mean NO₃⁻ concentrations for snowpits are shown in Fig. 1. ~~On~~ ~~From the coast to~~ ~~the coastal~~ ~450
313 km ~~inland~~, snowpit NO₃⁻ means are comparable to those of surface snow; whereas, NO₃⁻ means are
314 lower in inland snowpits than in surface snow with the exception of sites ~800 km from the coast. In
315 general, the differences between snowpit NO₃⁻ means and the corresponding surface snow values are
316 small at sites with high snow accumulation (e.g., close to coast), while the differences are large in low
317 snow accumulation areas (e.g., near Dome A).

318 The profiles of NO₃⁻ for all snowpits are shown in Fig. 3. NO₃⁻ concentrations vary remarkably with
319 depth in pits SP1 - SP5, which are located near the coast. Although SP2 and SP5 show high NO₃⁻
320 concentrations in the topmost sample, the data from deeper depths can be compared with the surface
321 values. In addition, NO₃⁻ means for the entire snowpits are close to the means of the topmost layer
322 covering a full annual cycle of accumulation (i.e., the most recent year of snow accumulation) at
323 SP1-SP5 (Fig. 4). Given the high snow accumulation (Fig. 1), NO₃⁻ variability in coastal snowpits is
324 likely suggestive of a seasonal signature (Wagenbach et al., 1998b; Grannas et al., 2007; Shi et al.,
325 2015). Among the coastal snowpits, water isotope ratios ($\delta^{18}\text{O}$ of H₂O) of samples at SP02 were also
326 determined, thus allowing for investigating NO₃⁻ seasonal variability (Fig. S3 in supporting
327 information). In general, the $\delta^{18}\text{O}$ (H₂O) peaks correspond to high NO₃⁻ concentrations (i.e., NO₃⁻ peaks
328 present in summer). This seasonal pattern is in agreement with previous observations of NO₃⁻ in
329 snow/ice and atmosphere in coastal Antarctica (Mulvaney and Wolff, 1993; Mulvaney et al., 1998;
330 Wagenbach et al., 1998b; Savarino et al., 2007).

331 In contrast, most of the inland snowpits show high NO₃⁻ concentrations in the top layer, and then fall
332 sharply from > 2.0 $\mu\text{eq L}^{-1}$ in top snow to < 0.2 $\mu\text{eq L}^{-1}$ in the first meter of depth (Fig. 3). NO₃⁻ means
333 for the entire snowpits are typically lower than those of the most recent year snow layer (Fig. 4).
334 Similar NO₃⁻ profiles for snowpits have been reported elsewhere in Antarctica, as a result of
335 post-depositional processing of NO₃⁻ (R  hlisberger et al., 2000; McCabe et al., 2007; Erbland et al.,
336 2013; Shi et al., 2015).

337 Comparison of the NO₃⁻ profile patterns reveals significant spatial heterogeneity, even for
338 neighboring sites. For instance, sites SP11 and SP12, 14 km apart, feature similar snow accumulation
339 rate (Table 1). If it is assumed that snow accumulation is relatively constant during the past several
340 years at SP11 (sampled in 2012/2013), snow in the depth of ~54 cm corresponds to the deposition in
341 2009/2010 (snow density = 0.45 g cm⁻³, from field measurements). NO₃⁻ concentrations are much
342 higher in the top snow of SP12 (sampled in 2009/2010) than in the depth of ~54 cm in SP11 (Fig. 3).
343 This variation in NO₃⁻ profiles at a local scale has been reported, possibly related to local morphologies
344 associated with sastrugi formation and wind drift (Frey et al., 2009; Traversi et al., 2009). It is
345 interesting that higher NO₃⁻ concentrations were not found in the uppermost layer at sites SP7 and SP8
346 (~600 km from coast; Fig. 3), where large sastrugi with hard smooth surfaces was extensively
347 developed (from field observations; Fig. S4 in supporting information). Snow accumulation rate in this
348 area fluctuates remarkably, and the values of some sites are rather small or close to zero due to the
349 strong wind scouring (Fig. 1) (Ding et al., 2011; Das et al., 2013). In this case, the snowpit NO₃⁻
350 profiles appear to be largely influenced by wind scour on snow, possibly resulting in missing years
351 and/or intra-annual mixing.

352

353 4 Discussion

354

355 4.1 Accumulation influence on NO₃⁻

356 The preservation of NO₃⁻ is thought to be closely associated with snow accumulation, where most of
357 the deposited NO₃⁻ is preserved at sites with higher snow accumulation (Wagenbach et al., 1994;
358 Hastings et al., 2004; Fibiger et al., 2013). Whereas, NO₃⁻ may be altered significantly at sites with low
359 snow accumulation, largely due to photolysis (Blunier et al., 2005; Grannas et al., 2007; Frey et al.,
360 2009; Erbland et al., 2013; Erbland et al., 2015). In the following discussion, we divide the traverse
361 into two zones, i.e., the coastal zone (<~450 km from the coast, including SP1-SP5 and Core 1; Table
362 1) and the inland region (~450 km to Dome A, including pits SP6-SP20 and Core 2; Table 1), following
363 NO₃⁻ distribution patterns in surface snow and snowpits (sections 3.1 and 3.2) as well as the spatial
364 pattern of snow accumulation rate (Fig. 1).

365 As for snowpits, NO₃⁻ levels in top and deeper layers are comparable near the coast, while NO₃⁻
366 differs considerably between the upper and deeper snow at inland sites (Figs. 3 and 4). ~~It is~~
367 ~~demonstrated that p~~ photochemical processing is responsible for NO₃⁻ distribution in inland snowpits
368 (Erbland et al., 2013; Berhanu et al., 2015). Considering that the actinic flux is always negligible below
369 the depth of 1 m, the bottom layers of the snowpits (i.e., > 100 cm; Table 1) are well below the
370 photochemically active zone (France et al., 2011; Zatko et al., 2013). In this case, NO₃⁻ in the bottom
371 snowpit, i.e., below the photic zone, can be taken as the archived fraction without further modification,
372 ~~as also suggested by on the basis of~~ previous observations (Frey et al., 2009; Erbland et al., 2013;
373 Erbland et al., 2015). Here, we define NO₃⁻ in the bottom layer covering a full annual cycle of
374 deposition as an approximation of the annual mean of archived NO₃⁻ (i.e., beyond photochemical
375 processing; denoted as “C_{archived}” in the following context; Fig. 4), thus allowing for calculating the
376 archived annual NO₃⁻ flux (i.e., the product of C_{archived} and annual snow accumulation rate). Although
377 there is uncertainty ~~over in~~ the calculation of archived NO₃⁻ flux due to interannual variability in NO₃⁻
378 inputs and snow accumulation, this assumption provides a useful way to investigate the relationship
379 between preservation of NO₃⁻ and physical factors considering that an extensive array of ice core
380 measurements is unavailable in most of Antarctica. It is noted that C_{archived} is generally close to (lower
381 than) the NO₃⁻ means for entire snowpits in coastal (inland) Antarctica (Fig. 4).

382 383 4.1.1 NO₃⁻ in coastal snowpack

384 The simplest plausible model to relate flux and concentration of NO₃⁻ in snow to its atmospheric
385 concentration (Legrand, 1987; Alley et al., 1995) can be expressed as,

$$386 F_{\text{total}} = K_1 C_{\text{atm}} + K_2 C_{\text{atm}} A \text{ (Eq. 4),}$$

$$387 F_{\text{total}} = C_{\text{firm}} \times A \text{ (Eq. 5),}$$

388 where F_{total} is snow NO₃⁻ flux ($\mu\text{eq m}^{-2} \text{ a}^{-1}$); C_{atm} is atmospheric concentration of NO₃⁻ ($\mu\text{eq m}^{-3}$); A is
389 annual snow accumulation rate ($\text{kg m}^{-2} \text{ a}^{-1}$); C_{firm} is measured firm NO₃⁻ concentration ($\mu\text{eq L}^{-1}$, here
390 $C_{\text{firm}} = C_{\text{archived}}$); K_1 is the dry deposition velocity (cm s^{-1}); and K_2 is the scavenging ratio for precipitation
391 ($\text{m}^3 \text{ kg}^{-1}$), which allows ~~to convert~~ conversion of atmospheric concentration to snow concentration of
392 NO₃⁻ in this study. From Eqs. 4 and 5, firm NO₃⁻ concentration can be expressed as,

$$393 C_{\text{firm}} = K_1 C_{\text{atm}} \times 1/A + K_2 C_{\text{atm}} \text{ (Eq. 6)}$$

394 If K_1 and K_2 are constants, a linear relationship between measured NO₃⁻ concentration (C_{firm}) and snow
395 accumulation (A) can be interpreted using Eq. 6, which assumes regional spatial homogeneity of fresh
396 snow NO₃⁻ levels and dry deposition flux ~~in the regions~~. The slope ($K_1 C_{\text{atm}}$) of the linear model
397 represents an approximation of dry deposition flux of NO₃⁻ (i.e., an apparent dry deposition flux), while
398 the intercept ($K_2 C_{\text{atm}}$) stands for NO₃⁻ concentration in fresh snowfall. If dry deposition ($K_1 C_{\text{atm}}$) is

399 much larger than wet deposition ($K_2 C_{\text{atm}} A$), the concentration of NO_3^- in snow will be proportional to
400 its concentration in the atmosphere. In the condition of a constant atmospheric concentration, larger
401 snow accumulation will increase the flux of NO_3^- but decrease its concentration in snow. While this
402 linear model is a gross over-simplification of the complex nature of air-snow exchange of NO_3^- , it
403 provides a simple approach to compare the processes occurring on the coast versus those inland. In
404 addition, this model can provide useful parameter values in modeling NO_3^- deposition/preservation at
405 large scales, considering that observations remain sparse across Antarctica (e.g., Zatzko et al., 2016).

406 The relationship between C_{archived} of NO_3^- and snow accumulation rate is shown in Fig. 5. The linear
407 fit of C_{archived} vs. inverse snow accumulation ($R^2=0.88$, $p<0.01$; Fig. 5a) supports the assumptions of
408 spatial homogeneity. The intercept and slope of the linear fit suggest a NO_3^- concentration in fresh
409 snow and an apparent NO_3^- dry deposition flux of $0.7 \pm 0.07 \mu\text{eq L}^{-1}$ and $45.7 \pm 7.8 \mu\text{eq m}^{-2} \text{a}^{-1}$
410 respectively. The apparent dry deposition flux is opposite to the observation in Dronning Maud Land
411 (DML) region, where the negative dry deposition flux suggested net losses of NO_3^- (Pasteris et al.,
412 2014).

413 Figure 5b shows the archived fluxes of NO_3^- on the coast, with values from 104 (at the lowest
414 accumulation site) to $169 \mu\text{eq m}^{-2} \text{a}^{-1}$ (at the highest accumulation site). Taking the calculated NO_3^- dry
415 deposition flux of $45.7 \mu\text{eq m}^{-2} \text{a}^{-1}$, dry deposition accounts for 27-44 % (mean = 36 %) of total NO_3^-
416 inputs, with higher (lower) percentages at lower (higher) snow accumulation sites. This result is in line
417 with the observations in Taylor Valley (coastal West Antarctica), where the snowfall was found to be
418 the primary driver for NO_3^- inputs (Witherow et al., 2006). This observation also generally agrees with,
419 but is greater than that in the modeling study of Zatzko et al. (2016), which predicts a ratio of dry
420 deposition to total deposition of NO_3^- in Antarctica as $< 20\%$ close to the coast, increasing towards the
421 plateaus.

422 In Figs. 5a and b, the strong linear relationships between NO_3^- and snow accumulation support that
423 K_1 and K_2 are relatively constant on the coast (Eqs. 4 and 6). The average atmospheric concentration of
424 NO_3^- in the coastal ~450 km region is 19.4 ng m^{-3} in summer (Table S1 in supporting information).
425 Taking $C_{\text{atm}}=19.4 \text{ ng m}^{-3}$, K_1 is estimated to be 0.5 cm s^{-1} , identical to a typical estimate for HNO_3
426 deposition velocity to a snow/ice surface (0.5 cm s^{-1} ; Seinfeld and Pandis, 1997). This predicted K_1
427 value is lower than that calculated for the dry deposition of HNO_3 at South Pole (0.8 cm s^{-1} ; Huey et al.,
428 2004). It is noted that the true K_1 value could be larger than the prediction (0.5 cm s^{-1}) due to the higher
429 values of C_{atm} atmospheric NO_3^- concentrations during in summer (i.e., 19.4 ng m^{-3} for the calculation
430 of K_1 time than in other seasons (Mulaney et al., 1998; Wagenbach et al., 1998b; Savarino et al.,
431 2007). The scavenging ratio for precipitation (K_2) is calculated to be $0.2 \times 10^4 \text{ m}^3 \text{ kg}^{-1}$, i.e., $2 \text{ m}^3 \text{ g}^{-1}$.

432 If it is assumed that NO_3^- concentration in snow is related to its concentration in the atmosphere, the
433 scavenging ratio for NO_3^- (W) can be calculated on a mass basis from the following expression
434 (Kasper-Giebl et al., 1999),

$$W = \rho_{\text{atm}} \times (C_{\text{f-snow}} / C_{\text{atm}}) \text{ (Eq. 7)},$$

435 where ρ_{atm} is air density (g m^{-3}), and $C_{\text{f-snow}}$ and C_{atm} are NO_3^- concentrations in fresh snow (ng g^{-1}) and
436 atmosphere (ng m^{-3}) respectively. If taking $\rho_{\text{atm}} \approx 1000 \text{ g m}^{-3}$ (on average, ground surface temperature t
437 $\approx 255 \text{ K}$, ground pressure $P \approx 0.08 \text{ MPa}$, in the coastal region), $C_{\text{f-snow}} = 43 \text{ ng g}^{-1}$ (see discussion above
438 and section 4.2 below), and $C_{\text{atm}} = 19.4 \text{ ng m}^{-3}$, W is calculated to be ~ 2200 , generally comparable to
439 previous reports (Barrie, 1985; Kasper-Giebl et al., 1999; Shrestha et al., 2002). It is noted that the
440 calculation here may be subject to uncertainty, due to the complex transfer of atmospheric NO_3^- into the
441 snow. However, the scavenging ratio provides useful-valuable insights into the relation between NO_3^-
442

443 concentrations in the atmosphere and snow, which might be useful in modeling NO_3^- deposition at a
444 large-scale.

445 Figure 5c shows the distribution of flux is negatively correlated with C_{archived} of NO_3^- , which is not
446 surprising since C_{archived} is positively related to inverse accumulation (Fig. 5a). Based on the observed
447 strong linear relationship between NO_3^- flux and snow accumulation (Fig. 5b), the archived NO_3^- flux
448 is more accumulation dependent compared to C_{archived} . This is compatible with the observations in
449 Greenland (Burkhart et al., 2009), where accumulation is generally above $100 \text{ kg m}^{-2} \text{ a}^{-1}$, similar to the
450 coastal values in this study.

451 In terms of surface snow on the coast, NO_3^- may be disturbed by the katabatic winds and wind
452 convergence located near the Amery Ice Shelf (that is, the snow-sourced NO_x and NO_3^- from the
453 Antarctic plateau possibly contributes to coastal snow NO_3^-) (Parish and Bromwich, 2007; Ma et al.,
454 2010; Zatko et al., 2016). In addition, the sampled ~3 cm surface layer roughly corresponds to the net
455 accumulation in the past 0.5-1.5 months assuming an even distribution of snow accumulation in the
456 course of a single year. This difference in exposure time of the surface snow at different sampling sites,
457 could possibly affect the concentration of NO_3^- , although the post-depositional alteration of NO_3^- was
458 thought to be minor on the coast (Wolff et al., 2008; Erbland et al., 2013; Shi et al., 2015). Taken
459 together, NO_3^- in coastal surface snow might represent some post-depositional alteration. Even so, a
460 negative correlation between NO_3^- concentration and snow accumulation rate was found at the coast
461 ($R^2=0.42$, $p<0.01$; Fig. 6a), suggesting that overall the majority of the NO_3^- appears to be preserved and
462 is driven-determined by snow accumulation.

463

464 4.1.2 NO_3^- in inland snowpack

465 In comparison with the coast, the correlation between C_{archived} and inverse snow accumulation is
466 relatively weak in inland regions (Fig. 5d), suggesting more variable conditions in ambient
467 concentrations and dry deposition flux of NO_3^- . In addition, the relationship of C_{archived} vs. inverse
468 accumulation—in inland is opposite to that of coast. Based on current understanding of the
469 post-depositional processing of NO_3^- , the negative correlation between C_{archived} and inverse snow
470 accumulation (Fig. 5d) suggests losses of NO_3^- . The slope of the linear relationship indicates apparent
471 NO_3^- dry deposition flux of $-44.5 \pm 3.0 \mu\text{eq m}^{-2} \text{ a}^{-1}$, much larger than that of DML ($-22.0 \pm 2.8 \mu\text{eq m}^{-2}$
472 a^{-1}), where the snow accumulation is generally lower than $100 \text{ kg m}^{-2} \text{ a}^{-1}$ (Pasteris et al., 2014). At
473 Kohlen Station (an inland site in East Antarctica), with snow accumulation of $71 \text{ kg m}^{-2} \text{ a}^{-1}$, the
474 emission flux of NO_3^- is estimated to be $-22.9 \pm 13.7 \mu\text{eq m}^{-2} \text{ a}^{-1}$ (Weller and Wagenbach, 2007), which
475 is also smaller in comparison with this observation. Weller et al. (2004) proposed that loss rate of NO_3^-
476 does not depend on snow accumulation rate and the losses become insignificant at accumulation rates
477 above $100 \text{ kg m}^{-2} \text{ a}^{-1}$. Among the inland sites, SP10 and Core2 (~800 km from the coast), featured by
478 high snow accumulation rate ($> 100 \text{ kg m}^{-2} \text{ a}^{-1}$; Table 1 and Fig. 1), exhibit even higher values of
479 C_{archived} and archived fluxes of NO_3^- than those of the coastal sites. It is noted that ~~the~~-these two cases
480 influence the linear regression significantly (Fig. 5d). If the two sites are excluded, we can get a linear
481 regression with ~~the a~~-slope of $-27.7 \pm 9.2 \mu\text{eq m}^{-2} \text{ a}^{-1}$, which is comparable to previous reports in DML
482 (Pasteris et al., 2014).

483 The depths of inland snowpits cover ~~past~~ several to tens of years' snow accumulation, thus allowing
484 for directly investigating NO_3^- emission rate. The difference between NO_3^- concentrations in the snow
485 layer accumulated during the most recent year (Fig. 4) and in the snow accumulated during the year
486 before the most recent year can represent the loss rate of NO_3^- . If it is assumed that snow accumulation

487 rate is relatively constant during ~~past-recent~~ decades at specific-sites, on average, 36.7 ± 21.3 % of NO_3^-
488 (in $\mu\text{eq L}^{-1}$) was lost during one year, ~~with (the two sites (SP10 and Core2) with snow~~
489 ~~accumulation $>100 \text{ kg m}^{-2} \text{ a}^{-1}$ excluded from the calculation)~~. The percentages are generally higher at
490 the sites with lower snow accumulation rate. Together with snow accumulation rate, the emission flux
491 of NO_3^- is calculated to be $-28.1 \pm 23.0 \mu\text{eq m}^{-2} \text{ a}^{-1}$, close to the linear model prediction ($-27.7 \pm 9.2 \mu\text{eq}$
492 $\text{m}^{-2} \text{ a}^{-1}$). ~~The~~ Significant losses can account for NO_3^- profiles at inland sites, i.e., NO_3^- concentration
493 ~~decrease~~ decreasing with increasing depths. Previous observations and modeling works suggested that
494 photolysis dominates the losses (Frey et al., 2009; Erbland et al., 2013; Shi et al., 2015). During
495 photolysis of NO_3^- , some of the photoproducts (NO_x) are emitted into the gas phase (Davis et al., 2004;
496 France et al., 2011), and these products should undergo reoxidation by the local oxidants (e.g.,
497 hydroxyl radical (OH), $\text{NO}_2 + \text{OH} + \text{M} \rightarrow \text{HNO}_3 + \text{M}$), forming gas phase HNO_3 . In inland Antarctica,
498 the dominant NO_3^- species in the atmosphere is gaseous HNO_3 during summertime, while particulate
499 NO_3^- is more important in winter (Legrand et al., 2017b; Traversi et al., 2017). The high levels of gas
500 phase HNO_3 in summer support the importance of the re-emission from snow through the photolysis of
501 NO_3^- in affecting the atmospheric $\text{NO}_x/\text{NO}_3^-$ budget (Erbland et al., 2013). On the one hand, the
502 gaseous HNO_3 can be efficiently co-condensed with water vapour onto the extensively developed
503 crystal ice layers on Antarctic plateaus (e.g., Fig. S1 in supporting information ~~discussed above~~),
504 leading to an enrichment of NO_3^- in surface snow (Bock et al., 2016). On the other hand, a large
505 concentration of HNO_3 would enhance its reaction with sea-salt, leading to elevated particulate NO_3^-
506 concentrations (Legrand et al., 2017b). The significant correlation between NO_3^- and H^+ in inland
507 Antarctic surface snow ($R^2 = 0.65$, $p < 0.01$) seems to support the importance of atmospheric gas phase
508 HNO_3 in affecting surface snow NO_3^- concentrations, in particular NO_3^- levels in the crystal ice
509 samples (Fig. 1).

510 ~~Thus far,~~ Several modeling works have been performed to understand NO_3^- recycling processes
511 across Antarctica (e.g., Erbland et al., 2015; Zatko et al., 2016; Bock et al., 2016), however, ~~each~~
512 ~~employs different assumptions and large~~ uncertainty remains ~~about in quantifying~~ NO_3^- recycling and
513 preservation. It is thought that emission and transport strength are the ~~main~~ factors controlling the
514 recycling of NO_3^- , while the former is associated with initial NO_3^- concentrations, UV and snow optical
515 properties, and the latter is linked with air mass movement (Wolff et al., 2008; Frey et al., 2009). As a
516 result, snow accumulation alone is likely insufficient to account for NO_3^- variability in surface snow
517 (i.e., no significant correlation between NO_3^- concentration and snow accumulation; Fig. 6b).

518 The archived NO_3^- fluxes vary considerably among inland sites, from ~ 3 to $333 \mu\text{eq m}^{-2} \text{ a}^{-1}$, with
519 high values generally corresponding to high snow accumulation (Fig. 5e). However, the nearly 1:1
520 relationship between C_{archived} and NO_3^- flux (Fig. 5f), suggests that accumulation rate is not the main
521 driver of the archived NO_3^- concentration. In inland Antarctica, the archived NO_3^- fraction is largely
522 influenced by the length of time that NO_3^- was exposed to UV radiation (Berhanu et al., 2015), which
523 decreases exponentially in the snowpack. The e -folding depth, z_e value, is thought to be influenced by a
524 variety of factors, such as co-existent impurities (e.g., black carbon), bulk density and grain size (Zatko
525 et al., 2013). In addition, the snow albedo is also dependent on snow physical properties (Carmagnola
526 et al., 2013). Taken together, this suggests that the inland plateau is below a “threshold” of
527 accumulation rate such that the archived NO_3^- flux cannot be explained by snow accumulation rate.

528

529 4.2 Effects of coexisting ions on NO_3^-

530 Atmospheric NO_3^- in Antarctica is thought to be mainly associated with mid-latitude sources,

531 re-formed NO_3^- driven by snow-sourced photolysis products, and/or stratospheric inputs (Savarino et
532 al., 2007; Lee et al., 2014; Traversi et al., 2017 and references therein). [Although organic nitrates can](#)
533 [play an important role in the atmospheric \$\text{NO}_y\$ budget, multi-seasonal measurements of surface snow](#)
534 [\$\text{NO}_3^-\$ correlate strongly with inorganic \$\text{NO}_y\$ species \(especially \$\text{HNO}_3\$ \) rather than organic \(Jones et al.,](#)
535 [2011\). Here, ~~We~~ we investigate whether \$\text{NO}_3^-\$ in snow is closely associated with coexisting ions \(e.g., \$\text{Cl}^-\$,](#)
536 SO_4^{2-} , Na^+ , K^+ , Mg^{2+} and Ca^{2+}) since these ions have different main sources, e.g., Cl^- and Na^+ are
537 predominantly influenced by sea salt, and SO_4^{2-} is likely dominated by marine inputs (e.g., sea salt and
538 bio-activity source) (Bertler et al., 2005). In the snow, Cl^- , Na^+ and SO_4^{2-} are the most abundant ions in
539 addition to NO_3^- ~~and the potential association between NO_3^- and the three ions in the surface snow is~~
540 ~~discussed here.~~

541 In surface snow, the non-sea salt fraction of SO_4^{2-} ~~accounts~~ [accounted](#) for 75--99 % of its total
542 budget, with a mean of 95 %. The percentages ~~are~~ [were](#) relatively higher in inland regions than at
543 coastal sites. On the coast, a positive relationship was found between nssSO_4^{2-} and NO_3^- ($R^2 = 0.32$, $p <$
544 0.01 ; Fig. 7a). Previous observations suggest that NO_3^- and nssSO_4^{2-} peaks in the atmosphere and snow
545 are usually present in summer (Jourdain and Legrand, 2002; Wolff et al., 2008; Sigl et al., 2016;
546 Legrand et al., 2017a; Legrand et al., 2017b). However, the similar seasonal pattern of the two species
547 is associated with distinct sources, i.e., SO_4^{2-} is mainly derived from marine biogenic emissions while
548 NO_3^- is influenced by photolysis and tropospheric transport (Savarino et al., 2007; Lee et al., 2014;
549 Zatko et al., 2016). In the atmosphere, ~~most of~~ SO_4^{2-} is [typically found](#) on the submicron particles,
550 while most of ~~the~~ NO_3^- is gaseous HNO_3 and the particulate NO_3^- is mainly on ~~the~~ intermediate size
551 particles (Jourdain and Legrand, 2002; Rankin and Wolff, 2003; Legrand et al., 2017a; Legrand et al.,
552 2017b). Thus, the correlation between NO_3^- and SO_4^{2-} is unlikely explained by the sources or their
553 occurrence state in the atmosphere (i.e., gaseous and particulate phases). Laluraj et al. (2010) proposed
554 that the correlation between nssSO_4^{2-} vs. NO_3^- in ice ($R^2 = 0.31$, $p < 0.01$) could be associated with ~~the~~
555 ~~fine~~ nssSO_4^{2-} aerosols, which ~~could~~ provide nucleation centers forming ~~the~~ multi-ion complexes with
556 HNO_3 in the atmosphere. This assertion, however, should be examined further, considering that the
557 complex chemistry of SO_4^{2-} and NO_3^- in the atmosphere is far from understood (e.g., Wolff, 1995;
558 Brown et al., 2006). Thus far, the mechanism of nssSO_4^{2-} influencing NO_3^- in the snowpack, however,
559 is still debated, and it cannot be ruled out that nssSO_4^{2-} further affects mobilization of NO_3^- during
560 and/or after crystallization (Legrand and Kirchner, 1990; Wolff, 1995; R hlisberger et al., 2000). It is
561 noted that no relationship was found between nssSO_4^{2-} and NO_3^- in inland snow (Fig. 7d), possibly due
562 to the strong alteration of NO_3^- during post-depositional processes, as discussed in section 4.1.2.

563 In comparison with nssSO_4^{2-} aerosols, the sea-salt aerosols (Na^+) are coarser and can be removed
564 preferentially from the atmosphere due to a larger dry deposition velocity. High atmospheric sea salt
565 aerosol concentrations are expected to promote the conversion of gaseous HNO_3 to ~~the~~ particulate
566 phase, considering that most of the NO_3^- in the atmosphere is in the gas phase (HNO_3). In this case,
567 particulate NO_3^- can be efficiently lost via aerosol mechanisms. In addition, the saline ice also favors
568 the direct uptake of gaseous HNO_3 to the ice surface. Changes in partitioning between gas phase
569 (HNO_3) and particulate phase will affect NO_3^- levels due to the different wet and dry deposition rates of
570 the two species (Aw and Kleeman, 2003). Thus, sea salt aerosols play an important role in the
571 scavenging of gaseous HNO_3 from the atmosphere (Hara et al., 2005), and elevated NO_3^-
572 concentrations are usually accompanied by Na^+ spikes in ~~the~~ snowpack (e.g., at Halley station, ~~a~~
573 ~~coastal site~~; Wolff et al., 2008). [Here Surprisingly](#), no significant correlation was found between Na^+
574 and NO_3^- in coastal snow (Fig. 7b). The concentration profiles of NO_3^- and Na^+ in coastal surface snow

575 are shown in Fig. 8, and NO_3^- roughly corresponds to Na^+ in some areas, e.g., 50-150 km and 300-450
576 km distance inland, although in general they are not very coherent. It is noted that amongst the 4 snow
577 samples with $\text{Na}^+ > 1.5 \mu\text{eq L}^{-1}$ (open circles in Fig. 8), only one sample co-exhibits a NO_3^- spike. This
578 is different from observations at Halley station, where Na^+ peaks usually led to elevated NO_3^- levels in
579 surface snow in summer (Wolff et al., 2008). Of the 4 largest Na^+ spikes, one is a fresh snowfall sample
580 (dashed ellipse in Fig. 8), and this sample shows the highest Na^+ concentration ($2.8 \mu\text{eq L}^{-1}$) and low
581 NO_3^- ($0.75 \mu\text{eq L}^{-1}$). It is noted that NO_3^- concentration in this fresh snowfall is close to the model
582 predictions ($0.7 \pm 0.07 \mu\text{eq L}^{-1}$; section 4.1.1), validating that the simple linear deposition model (i.e., the
583 Eq. 6) can well depict the deposition and preservation of NO_3^- in coastal snowpack. At inland sites, no
584 correlation was found between NO_3^- and Na^+ (Fig. 7e), likely explained by the alteration of NO_3^-
585 concentration by post-depositional processing (discussed above).

586 In surface snow, nssCl^- represents 0-64 % (mean = 40 %) of the total Cl^- . On the coast, it is of
587 interest that nssCl^- in the 4 samples with the highest Na^+ concentrations (open circles in Figs. 7b and 8)
588 are close to 0, and positive nssCl^- values were found for the other samples. The fractionation of Na^+ can
589 occur due to mirabilite precipitation in sea-ice formation at $< -8^\circ\text{C}$ (Marion et al., 1999), possibly
590 leading to the positive nssCl^- . However, even if all of SO_4^{2-} in sea water is removed via mirabilite
591 precipitation, only 12 % of sea salt Na^+ is lost (Rankin et al., 2002). Considering the smallest sea ice
592 extent in summertime in East Antarctica (Holland et al., 2014), the high Cl^-/Na^+ ratio (mean = 2.1, well
593 above 1.17 of sea water, in $\mu\text{eq L}^{-1}$) in surface snow is unlikely from sea salt fractionation associated
594 with mirabilite precipitation in sea-ice formation. In this case, nssCl^- could be mainly related to the
595 deposition of volatile HCl , which is from the reaction of H_2SO_4 and/or HNO_3 with NaCl (R hlisberger
596 et al., 2003). In this case Thus, nssCl^- in snowpack can roughly represent the atmospherically deposited
597 HCl . In the summertime, most of the dechlorination (i.e., production of HCl) is likely associated with
598 HNO_3 due to its high atmospheric concentrations (Jourdain and Legrand, 2002; Legrand et al., 2017b).
599 Thus Accordingly, the observed relationship between NO_3^- and nssCl^- (Fig. 7c) appears to suggest that
600 HCl production can be enhanced by elevated HNO_3 levels in the atmosphere.

601 With regard to the crystal ice, no significant correlation was found between NO_3^- and the coexisting
602 ions (e.g., Cl^- , Na^+ and SO_4^{2-}), suggesting that these ions are generally less influential on NO_3^- in this
603 uppermost thin layer, compared to the strong air-snow transfer process of NO_3^- (Erblant et al., 2013). It
604 is noted that NO_3^- accounts for most of the calculated H^+ concentrations (81–97 %, mean = 89 %), and
605 a strong linear relationship was found between them ($R^2 = 0.96$, $p < 0.01$), suggesting that NO_3^- is mainly
606 deposited as acid, HNO_3 , rather than in particulate form as salts (e.g., NaNO_3 and $\text{Ca}(\text{NO}_3)_2$). This
607 deduction is in line with the atmospheric observations at Dome C, where NO_3^- was found to be mainly
608 in gaseous phase (HNO_3) in summer (Legrand et al., 2017b). On average, the deposition of HNO_3
609 contributes > 91 % of NO_3^- in the crystal ice (the lower limit, 91 %, calculated by assuming all of the
610 alkaline species (Na^+ , NH_4^+ , K^+ , Mg^{2+} and Ca^{2+}) are neutralized by HNO_3 in the atmosphere),
611 suggesting a dominant role of HNO_3 deposition in snow NO_3^- concentrations. The elevated high
612 atmospheric NO_3^- concentrations observed at Dome A ($> 100 \text{ ng m}^{-3}$; 77.12°E and 80.42°S , Table S1 in
613 supporting information) possibly indicate oxidation of gaseous NO_x to HNO_3 , providing further
614 evidence that NO_3^- recycling driven by photolysis plays an important role in its abundance in snowpack
615 on East Antarctic plateaus.

616

617 5 Conclusions

618 Samples of surface snow, snowpits and the uppermost layer of crystal ice, collected on the traverse

619 from the coast to Dome A, East Antarctica, were used to investigate the deposition and preservation of
620 NO_3^- in snow. In general, a spatial trend of NO_3^- in surface snow was found on the traverse, with high
621 (low) concentrations on the plateau (coast). Similarly, NO_3^- concentrations in the atmosphere are higher
622 on the plateau than at coastal sites, with a range of 8 to 183 ng m^{-3} . Extremely high NO_3^- levels (e.g., >
623 10 $\mu\text{eq L}^{-1}$) were observed in the uppermost crystal ice layer, possibly associated with re-deposition of
624 ~~the~~ recycled NO_3^- from snow-sourced NO_3^- . As for the snowpits, NO_3^- exhibits high levels in the top
625 layer and low concentrations at deeper depths in the inland region, while no clear trend was found on
626 the coast.

627 On the coast, the archived NO_3^- flux in snow is positively correlated with snow accumulation rate,
628 but negatively with NO_3^- concentration. A linear model can well depict the relationship between
629 archived NO_3^- and snow accumulation, supporting that atmospheric levels and dry deposition fluxes of
630 NO_3^- are spatially homogeneous on the coast, and that dry deposition plays a minor role in snow NO_3^-
631 inputs. The dry deposition velocity and scavenging ratio for NO_3^- are estimated to be 0.5 cm s^{-1} and
632 2200, respectively. In inland Antarctica, the archived NO_3^- fluxes, varying significantly among sites, are
633 largely dependent on NO_3^- concentration. A weak correlation between snow accumulation and archived
634 NO_3^- suggests variable ambient concentrations and dry deposition flux of NO_3^- , and the relationship is
635 opposite to that for the coast. This supports the idea that post-depositional processing dominates NO_3^-
636 concentration and distribution in inland Antarctica (e.g., Erbland et al., 2013; Erbland et al., 2015; Shi
637 et al., 2015; Zatko et al., 2016).

638 The major ions, Cl^- , SO_4^{2-} and Na^+ , originate from different sources ~~from~~ than NO_3^- , but could
639 potentially affect the scavenging and preservation of NO_3^- . In coastal surface snow, a positive
640 correlation between nssSO_4^{2-} and NO_3^- suggests the potential influence of fine aerosols on NO_3^-
641 formation and/or scavenging, while the coarse sea salt aerosol (e.g., Na^+) is likely less influential. In
642 contrast to the coast, NO_3^- in inland surface snow is dominated by post-depositional processes, and the
643 effects of coexisting ions on NO_3^- appear to be rather minor. In inland surface snow, the strong
644 relationship between NO_3^- and H^+ suggests a dominant role of gaseous HNO_3 deposition in determining
645 NO_3^- concentrations.

646

647 **Associated content**

648 Please see the file of Supporting Information.

649

650 **Acknowledgement**

651 This project was supported by the National Science Foundation of China (Grant nos. 41576190 and
652 41206188 to GS, 41476169 to SJ), the National Key Research and Development Program of China
653 (Grant no. 2016YFA0302204), the Fundamental Research Funds for the Central Universities (Grant No
654 40500-20101-222006), and Chinese Polar Environment Comprehensive Investigation and Assessment
655 Programmes (Grant nos. CHINARE 201X-02-02 and 201X-04-01). The authors appreciate the
656 CHINARE inland members for providing help during sampling. The authors would like to thank Prof.
657 Joel Savarino and two anonymous referees for their help in the development and improvement of this
658 paper.

659

660 **References**

661 Alexander, B., Savarino, J., Kreutz, K.J., and Thiemens, M.: Impact of preindustrial biomass-burning
662 emissions on the oxidation pathways of tropospheric sulfur and nitrogen, *J. Geophys. Res.*, 109,

663 D08303, doi:10.1029/2003JD004218, 2004.

664 Alley, R., Finkel, R., Nishizumi, K., Anandakrishnan, A., Shuman, C., Mershon, G., Zielinski, G., and
665 Mayewski, P.A.: Changes in continental and sea-salt atmospheric loadings in central Greenland during
666 the most recent deglaciation: Model-based estimates, *J. Glaciol.*, **41**, 503-514, 1995.

667 Arthern, R.J., Winebrenner, D.P., and Vaughan, D.G.: Antarctic snow accumulation mapped using
668 polarization of 4.3-cm wavelength microwave emission, *J. Geophys. Res.*, **111**,
669 doi:10.1029/2004JD005667, 2006.

670 Aw, J., and Kleeman, M.J.: Evaluating the first-order effect of intraannual temperature variability on
671 urban air pollution, *J. Geophys. Res.*, **108**, -, 2003.

672 Barrie, L.A.: Scavenging ratios, wet deposition, and in-cloud oxidation: An application to the oxides of
673 sulphur and nitrogen, *J. Geophys. Res.*, **90**, 5789–5799, 1985.

674 Berhanu, T.A., Meusinger, C., Erbland, J., Jost, R., Bhattacharya, S., Johnson, M.S., and Savarino, J.:
675 Laboratory study of nitrate photolysis in Antarctic snow. II. Isotopic effects and wavelength
676 dependence, *J. Chem. Phys.*, **140**, 244306, doi:10.1063/1.4882899, 2014.

677 Berhanu, T.A., Savarino, J., Erbland, J., Vicars, W.C., Preunkert, S., Martins, J.F., and Johnson, M.S.:
678 Isotopic effects of nitrate photochemistry in snow: a field study at Dome C, Antarctica, *Atmos. Chem.*
679 *Phys.*, **15**, 11243-11256, doi:10.5194/acp-15-11243-2015, 2015.

680 Bertler, N., Mayewski, P.A., Aristarain, A., Barrett, P., Becagli, S., Bernardo, R., Bo, S., Xiao, C., Curran,
681 M., and Qin, D.: Snow chemistry across Antarctica, *Ann. Glaciol.*, **41**, 167-179, 2005.

682 Blunier, T., Floch, G., Jacobi, H.-W., and Quansah, E.: Isotopic view on nitrate loss in Antarctic surface
683 snow, *Geophys. Res. Lett.*, **32**, L13501, doi:10.1029/2005GL023011, 2005.

684 Bock, J., Savarino, J., and Picard, G.: Air–snow exchange of nitrate: a modelling approach to investigate
685 physicochemical processes in surface snow at Dome C, Antarctica, *Atmos. Chem. Phys.*, **16**,
686 12531-12550, doi:10.5194/acp-16-12531-2016, 2016.

687 Brown, S., Ryerson, T., Wollny, A., Brock, C., Peltier, R., Sullivan, A., Weber, R., Dube, W., Trainer, M.,
688 and Meagher, J.: Variability in nocturnal nitrogen oxide processing and its role in regional air quality,
689 *Science*, **311**, 67-70, doi:10.1126/science.1120120, 2006.

690 Burkhart, J.F., Bales, R.C., McConnell, J.R., Hutterli, M.A., and Frey, M.M.: Geographic variability of
691 nitrate deposition and preservation over the Greenland Ice Sheet, *J. Geophys. Res.*, **114**,
692 doi:10.1029/2008JD010600, 2009.

693 Carmagnola, C., Domine, F., Dumont, M., Wright, P., Strellis, B., Bergin, M., Dibb, J., Picard, G., and
694 Morin, S.: Snow spectral albedo at Summit, Greenland: measurements and numerical simulations
695 based on physical and chemical properties of the snowpack, *The Cryosphere*, **7**, 1139-1160,
696 doi:10.5194/tc-7-1139-2013, 2013.

697 Das, I., Bell, R.E., Scambos, T.A., Wolovick, M., Creyts, T.T., Studinger, M., Frearson, N., Nicolas, J.P.,
698 Lenaerts, J.T., and van den Broeke, M.R.: Influence of persistent wind scour on the surface mass
699 balance of Antarctica, *Nat. Geosci.*, **6**, 367-371, doi:10.1038/NGEO1766, 2013.

700 Davis, D., Chen, G., Buhr, M., Crawford, J., Lenschow, D., Lefer, B., Shetter, R., Eisele, F., Mauldin, L., and
701 Hogan, A.: South Pole NO_x chemistry: an assessment of factors controlling variability and absolute
702 levels, *Atmos. Environ.*, **38**, 5375-5388, doi:10.1016/j.atmosenv.2004.04.039, 2004.

703 Dibb, J.E., Gregory Huey, L., Slusher, D.L., and Tanner, D.J.: Soluble reactive nitrogen oxides at South
704 Pole during ISCAT 2000, *Atmos. Environ.*, **38**, 5399-5409, doi:10.1016/j.atmosenv.2003.01.001, 2004.

705 Ding, M., Xiao, C., Jin, B., Ren, J., Qin, D., and Sun, W.: Distribution of $\delta^{18}\text{O}$ in surface snow along a
706 transect from Zhongshan Station to Dome A, East Antarctica, *Chin. Sci. Bull.*, **55**, 2709-2714,

707 doi:10.1007/s11434-010-3179-3, 2010.

708 Ding, M., Xiao, C., Li, Y., Ren, J., Hou, S., Jin, B., and Sun, B.: Spatial variability of surface mass balance
709 along a traverse route from Zhongshan station to Dome A, Antarctica, *J. Glaciol.*, 57, 658-666, 2011.

710 Duderstadt, K.A., Dibb, J.E., Jackman, C.H., Randall, C.E., Solomon, S.C., Mills, M.J., Schwadron, N.A.,
711 and Spence, H.E.: Nitrate deposition to surface snow at Summit, Greenland, following the 9 November
712 2000 solar proton event, *J. Geophys. Res.*, 119, 6938-6957, 2014.

713 Duderstadt, K.A., Dibb, J.E., Schwadron, N.A., Spence, H.E., Solomon, S.C., Yudin, V.A., Jackman, C.H.,
714 and Randall, C.E.: Nitrate ion spikes in ice cores not suitable as proxies for solar proton events, *J.*
715 *Geophys. Res.*, 121, 2994-3016, doi:10.1002/2015JD023805, 2016.

716 Erbland, J., Savarino, J., Morin, S., France, J.L., Frey, M.M., and King, M.D.: Air-snow transfer of nitrate
717 on the East Antarctic plateau -Part 2: An isotopic model for the interpretation of deep ice-core records,
718 *Atmos. Chem. Phys.*, 15, 12079–12113, doi:10.5194/acp-15-12079-2015, 2015.

719 Erbland, J., Vicars, W., Savarino, J., Morin, S., Frey, M., Frosini, D., Vince, E., and Martins, J.: Air-snow
720 transfer of nitrate on the East Antarctic Plateau - Part 1: Isotopic evidence for a photolytically driven
721 dynamic equilibrium in summer, *Atmos. Chem. Phys.*, 13, 6403-6419, doi:10.5194/acp-13-6403-2013,
722 2013.

723 Felix, J.D., and Elliott, E.M.: The agricultural history of human - nitrogen interactions as recorded in ice
724 core $\delta^{15}\text{N} - \text{NO}_3^-$, *Geophys. Res. Lett.*, 40, 1642-1646, doi:10.1002/grl.50209, 2013.

725 Fibiger, D.L., Hastings, M.G., Dibb, J.E., and Huey, L.G.: The preservation of atmospheric nitrate in snow
726 at Summit, Greenland, *Geophys. Res. Lett.*, 40, 3484-3489, doi:10.1002/grl.50659, 2013.

727 France, J., King, M., Frey, M., Erbland, J., Picard, G., Preunkert, S., MacArthur, A., and Savarino, J.: Snow
728 optical properties at Dome C (Concordia), Antarctica; implications for snow emissions and snow
729 chemistry of reactive nitrogen, *Atmos. Chem. Phys.*, 11, 9787-9801, doi:10.5194/acp-11-9787-2011,
730 2011.

731 Frey, M.M., Savarino, J., Morin, S., Erbland, J., and Martins, J.: Photolysis imprint in the nitrate stable
732 isotope signal in snow and atmosphere of East Antarctica and implications for reactive nitrogen cycling,
733 *Atmos. Chem. Phys.*, 9, 8681-8696, 2009.

734 Geng, L., Alexander, B., Cole-Dai, J., Steig, E.J., Savarino, J., Sofen, E.D., and Schauer, A.J.: Nitrogen
735 isotopes in ice core nitrate linked to anthropogenic atmospheric acidity change, *Proc. Natl. Acad. Sci.*,
736 111, 5808-5812, doi:10.1073/pnas.1319441111, 2014.

737 Geng, L., Murray, L.T., Mickley, L.J., Lin, P., Fu, Q., Schauer, A.J., and Alexander, B.: Isotopic evidence of
738 multiple controls on atmospheric oxidants over climate transitions, *Nature*, 546, 133-136,
739 doi:10.1038/nature22340, 2017.

740 Goodwin, I., De Angelis, M., Pook, M., and Young, N.: Snow accumulation variability in Wilkes Land,
741 East Antarctica, and the relationship to atmospheric ridging in the 130° - 170° E region since 1930, *J.*
742 *Geophys. Res.*, 108, doi:10.1029/2002JD002995 2003.

743 Grannas, A., Jones, A.E., Dibb, J., Ammann, M., Anastasio, C., Beine, H., Bergin, M., Bottenheim, J.,
744 Boxe, C., and Carver, G.: An overview of snow photochemistry: evidence, mechanisms and impacts,
745 *Atmos. Chem. Phys.*, 7, 4329-4373, 2007.

746 Hara, K., Osada, K., Kido, M., Matsunaga, K., Iwasaka, Y., Hashida, G., and Yamanouchi, T.: Variations of
747 constituents of individual sea-salt particles at Syowa station, Antarctica, *Tellus B*, 57, 230-246, 2005.

748 Hastings, M.G., Jarvis, J.C., and Steig, E.J.: Anthropogenic impacts on nitrogen isotopes of ice-core
749 nitrate, *Science*, 324, 1288-1288, doi:10.1126/science.1170510, 2009.

750 Hastings, M.G., Steig, E., and Sigman, D.: Seasonal variations in N and O isotopes of nitrate in snow at

751 Summit, Greenland: Implications for the study of nitrate in snow and ice cores, *J. Geophys. Res.*, 109,
752 D20306, doi:10.1029/2004JD004991, 2004.

753 Holland, P.R., Bruneau, N., Enright, C., Losch, M., Kurtz, N.T., and Kwok, R.: Modeled Trends in Antarctic
754 Sea Ice Thickness, *J. Climate*, 27, 3784-3801, doi:10.1175/JCLI-D-13-00301.1, 2014.

755 Hou, S., Li, Y., Xiao, C., and Ren, J.: Recent accumulation rate at Dome A, Antarctica, *Chin. Sci. Bull.*, 52,
756 428-431, 2007.

757 Huey, L.G., Tanner, D.J., Slusher, D.L., Dibb, J.E., Arimoto, R., Chen, G., Davis, D., Buhr, M.P., Nowak, J.B.,
758 Mauldin Iii, R.L., Eisele, F.L., and Kosciuch, E.: CIMS measurements of HNO₃ and SO₂ at the South Pole
759 during ISCAT 2000, *Atmos. Environ.*, 38, 5411-5421, doi:10.1016/j.atmosenv.2004.04.037, 2004.

760 Jones, A.E., Weller, R., Minikin, A., Wolff, E.W., Sturges, W.T., McIntyre, H.P., Leonard, S.R., Schrems, O.,
761 and Bauguitte, S.: Oxidized nitrogen chemistry and speciation in the Antarctic troposphere, *J. Geophys.*
762 *Res.*, 1042, 21355-21366, 1999.

763 Jones, A.E., Wolff, E.W., Ames, D., Bauguitte, S.-B., Clemmshaw, K., Fleming, Z., Mills, G., Saiz-Lopez, A.,
764 Salmon, R.A., and Sturges, W.: The multi-seasonal NO_y budget in coastal Antarctica and its link with
765 surface snow and ice core nitrate: results from the CHABLIS campaign, *Atmos. Chem. Phys.*, 11,
766 9271-9285, 2011.

767 Jourdain, B., and Legrand, M.: Year - round records of bulk and size - segregated aerosol composition
768 and HCl and HNO₃ levels in the Dumont d'Urville (coastal Antarctica) atmosphere: Implications for
769 sea - salt aerosol fractionation in the winter and summer, *J. Geophys. Res.*, 107, ACH 20-21 - ACH
770 20-13, doi:10.1029/2002JD002471, 2002.

771 Kasper-Giebl, A., Kalina, M.F., and Puxbaum, H.: Scavenging ratios for sulfate, ammonium and nitrate
772 determined at Mt. Sonnblick (3106m a.s.l.), *Atmos. Environ.*, 33, 895-906, 1999.

773 Laluraj, C., Thamban, M., Naik, S., Redkar, B., Chaturvedi, A., and Ravindra, R.: Nitrate records of a
774 shallow ice core from East Antarctica: Atmospheric processes, preservation and climatic implications,
775 *The Holocene*, 21, 351-356, doi:10.1177/0959683610374886, 2010.

776 Lee, H.-M., Henze, D.K., Alexander, B., and Murray, L.T.: Investigating the sensitivity of surface-level
777 nitrate seasonality in Antarctica to primary sources using a global model, *Atmos. Environ.*, 89, 757-767,
778 doi:10.1016/j.atmosenv.2014.03.003, 2014.

779 Legrand, M.: Chemistry of Antarctic snow and ice, *Le Journal De Physique Colloques*, 48, C1-77-C71-86,
780 1987.

781 Legrand, M., and Kirchner, S.: Origins and variations of nitrate in South Polar precipitation, *J. Geophys.*
782 *Res.*, 95, 3493-3507 1990.

783 Legrand, M., and Mayewski, P.A.: Glaciochemistry of polar ice cores: a review, *Rev. Geophys.*, 35,
784 219-243, 1997.

785 Legrand, M., Preunkert, S., Weller, R., Zipf, L., Elsässer, C., Merchel, S., Rugel, G., and Wagenbach, D.:
786 Year-round record of bulk and size-segregated aerosol composition in central Antarctica (Concordia
787 site) – Part 2: Biogenic sulfur (sulfate and methanesulfonate) aerosol, *Atmos. Chem. Phys.*, 17,
788 14055-14073, doi:10.5194/acp-17-14055-2017, 2017a.

789 Legrand, M., Preunkert, S., Wolff, E., Weller, R., Jourdain, B., and Wagenbach, D.: Year-round records of
790 bulk and size-segregated aerosol composition in central Antarctica (Concordia site) – Part 1:
791 Fractionation of sea-salt particles, *Atmos. Chem. Phys.*, 17, 14039-14054,
792 doi:10.5194/acp-17-14039-2017, 2017b.

793 Legrand, M., Wolff, E., and Wagenbach, D.: Antarctic aerosol and snowfall chemistry: implications for
794 deep Antarctic ice-core chemistry, *Ann. Glaciol.*, 29, 66-72, 1999.

795 Legrand, M.R., Stordal, F., Isaksen, I.S.A., and Rognerud, B.: A model study of the stratospheric budget
796 of odd nitrogen, including effects of solar cycle variations, *Tellus Series B-chemical & Physical*
797 *Meteorology*, 41B, 413–426, doi:10.1111/j.1600-0889.1989.tb00318.x, 1989.

798 Li, C., Ren, J., Qin, D., Xiao, C., Hou, S., Li, Y., and Ding, M.: Factors controlling the nitrate in the DT-401
799 ice core in eastern Antarctica, *Sci. China Ser. D*, doi:10.1007/s11430-012-4557-2, 2013.

800 Li, Y., Cole-Dai, J., and Zhou, L.: Glaciochemical evidence in an East Antarctica ice core of a recent (AD
801 1450-1850) neoglacial episode, *J. Geophys. Res.*, 114, doi:10.1029/2008JD011091, 2009.

802 Li, Z., Zhang, M., Qin, D., Xiao, C., Tian, L., Kang, J., and Li, J.: The seasonal variations of $\delta^{18}\text{O}$, Cl^- , Na^+ ,
803 NO_3^- and Ca^{2+} in the snow and firn recovered from Princess Elizabeth Land, Antarctica, *Chin. Sci. Bull.*,
804 44, 2270-2273, 1999.

805 Liss, P.S., Chuck, A.L., Turner, S.M., and Watson, A.J.: Air-sea gas exchange in Antarctic waters, *Antarct.*
806 *Sci.*, 16, 517-529, doi:10.1017/S0954102004002299, 2004.

807 Ma, Y., Bian, L., Xiao, C., Allison, I., and Zhou, X.: Near surface climate of the traverse route from
808 Zhongshan Station to Dome A, East Antarctica, *Antarct. Sci.*, 22, 443-459,
809 doi:10.1017/S0954102010000209, 2010.

810 Marion, G., Farren, R., and Komrowski, A.: Alternative pathways for seawater freezing, *Cold Reg. Sci.*
811 *Technol.*, 29, 259-266, 1999.

812 Mayewski, P.A., and Legrand, M.R.: Recent increase in nitrate concentration of Antarctic snow, *Nature*,
813 346, 258-260, 1990.

814 McCabe, J.R., Thiemens, M.H., and Savarino, J.: A record of ozone variability in South Pole Antarctic
815 snow: Role of nitrate oxygen isotopes, *J. Geophys. Res.*, 112, D12303, doi:10.1029/2006JD007822,
816 2007.

817 Mulvaney, R., Wagenbach, D., and Wolff, E.W.: Postdepositional change in snowpack nitrate from
818 observation of year-round near-surface snow in coastal Antarctica, *J. Geophys. Res.*, 103, 11021-11031,
819 1998.

820 Mulvaney, R., and Wolff, E.: Evidence for winter/spring denitrification of the stratosphere in the nitrate
821 record of Antarctic firn cores, *J. Geophys. Res.*, 98, 5213-5220, 1993.

822 Mulvaney, R., and Wolff, E.: Spatial variability of the major chemistry of the Antarctic ice sheet, *Ann.*
823 *Glaciol.*, 20, 440-447, 1994.

824 Parish, T.R., and Bromwich, D.H.: Reexamination of the near-surface airflow over the Antarctic
825 continent and implications on atmospheric circulations at high southern latitudes, *Mon. Weather. Rev.*,
826 135, 1961-1973, doi:10.1175/MWR3374.1, 2007.

827 Pasteris, D., McConnell, J.R., Edwards, R., Isaksson, E., and Albert, M.R.: Acidity decline in Antarctic ice
828 cores during the Little Ice Age linked to changes in atmospheric nitrate and sea salt concentrations, *J.*
829 *Geophys. Res.*, 119, 5640-5652, doi:10.1002/2013JD020377, 2014.

830 Piel, C., Weller, R., Huke, M., and Wagenbach, D.: Atmospheric methane sulfonate and non-sea-salt
831 sulfate records at the European Project for Ice Coring in Antarctica (EPICA) deep-drilling site in
832 Dronning Maud Land, Antarctica, *J. Geophys. Res.*, 111, -, 2006.

833 Qin, D., Zeller, E.J., and Dreschhoff, G.A.: The distribution of nitrate content in the surface snow of the
834 Antarctic Ice Sheet along the route of the 1990 International Trans-Antarctica Expedition, *J. Geophys.*
835 *Res.*, 97, 6277-6284, 1992.

836 Röthlisberger, R., Hutterli, M.A., Sommer, S., Wolff, E.W., and Mulvaney, R.: Factors controlling nitrate
837 in ice cores: Evidence from the Dome C deep ice core, *J. Geophys. Res.*, 105, 20565-20572, 2000.

838 Röthlisberger, R., Hutterli, M.A., Wolff, E.W., Mulvaney, R., Fischer, H., Bigler, M., Goto-Azuma, K.,

839 Hansson, M.E., Ruth, U., and Siggaard-Andersen, M.-L.: Nitrate in Greenland and Antarctic ice cores: A
840 detailed description of post-depositional processes, *Ann. Glaciol.*, 35, 209-216, 2002.

841 Röthlisberger, R., Mulvaney, R., Wolff, E.W., Hutterli, M.A., Bigler, M., De Angelis, M., Hansson, M.E.,
842 Steffensen, J.P., and Udisti, R.: Limited dechlorination of sea-salt aerosols during the last glacial period:
843 Evidence from the European Project for Ice Coring in Antarctica (EPICA) Dome C ice core, *J. Geophys.*
844 *Res.*, 108, 4526, doi:4510.1029/2003JD003604, 2003.

845 Rankin, A.M., and Wolff, E.W.: A year-long record of size-segregated aerosol composition at Halley,
846 Antarctica, *J. Geophys. Res.*, 108, -, 2003.

847 Rankin, A.M., Wolff, E.W., and Martin, S.: Frost flowers: Implications for tropospheric chemistry and ice
848 core interpretation, *J. Geophys. Res.*, 107, AAC 4-1–AAC 4-15, 2002.

849 Russell, A., McGregor, G., and Marshall, G.: 340 years of atmospheric circulation characteristics
850 reconstructed from an eastern Antarctic Peninsula ice core, *Geophys. Res. Lett.*, 33, L08702,
851 doi:08710.01029/02006GL025899, 2006.

852 Russell, A., McGregor, G.R., and Marshall, G.J.: An examination of the precipitation delivery
853 mechanisms for Dolleman Island, eastern Antarctic Peninsula, *Tellus Series A-dynamic Meteorology &*
854 *Oceanography*, 56, 501–513, 2004.

855 Savarino, J., Kaiser, J., Morin, S., Sigman, D.M., and Thiemens, M.H.: Nitrogen and oxygen isotopic
856 constraints on the origin of atmospheric nitrate in coastal Antarctica, *Atmos. Chem. Phys.*, 7,
857 1925-1945, 2007.

858 Seinfeld, J.H., and Pandis, S.N., 1997. *Atmospheric Chemistry and Physics: From Air Pollution to*
859 *Climate Change*, 2nd ed. Wiley, New York.

860 Shi, G., Buffen, A.M., Hastings, M.G., Li, C., Ma, H., Li, Y., Sun, B., An, C., and Jiang, S.: Investigation of
861 post-depositional processing of nitrate in East Antarctic snow: isotopic constraints on photolytic loss,
862 re-oxidation, and source inputs, *Atmos. Chem. Phys.*, 15, 9435–9453, doi:10.5194/acp-15-9435-2015,
863 2015.

864 Shi, G., Li, Y., Jiang, S., An, C., Ma, H., Sun, B., and Wang, Y.: Large-scale spatial variability of major ions
865 in the atmospheric wet deposition along the China Antarctica transect (31° N~ 69° S), *Tellus B*, 64,
866 17134, doi:10.3402/tellusb.v64i0.17134, 2012.

867 Shrestha, A., Wake, C., Dibb, J., and Whitlow, S.: Aerosol and Precipitation Chemistry at a Remote
868 Himalayan Site in Nepal, *Aerosol Science & Technology*, 36, 441-456, 2002.

869 Sigl, M., Fudge, T.J., Winstrup, M., Coledai, J., Ferris, D., McConnell, J.R., Taylor, K.C., Welten, K.C.,
870 Woodruff, T.E., and Adolphi, F.: The WAIS Divide deep ice core WD2014 chronology - Part 2:
871 Annual-layer counting (0-31 ka BP), *Clim. Past*, 11, 3425-3474, 2016.

872 Smart, D.F., Shea, M.A., Melott, A.L., and Laird, C.M.: Low time resolution analysis of polar ice cores
873 cannot detect impulsive nitrate events, *Journal of Geophysical Research: Space Physics*, 119,
874 9430-9440, doi:10.1002/2014JA020378, 2014.

875 Traversi, R., Becagli, S., Brogioni, M., Caiazza, L., Ciardini, V., Giardi, F., Legrand, M., Macelloni, G.,
876 Petkov, B., Preunkert, S., Scarchilli, C., Severi, M., Vitale, V., and Udisti, R.: Multi-year record of
877 atmospheric and snow surface nitrate in the central Antarctic plateau, *Chemosphere*, 172, 341-354,
878 doi:10.1016/j.chemosphere.2016.12.143, 2017.

879 Traversi, R., Becagli, S., Castellano, E., Cerri, O., Morganti, A., Severi, M., and Udisti, R.: Study of Dome
880 C site (East Antarctica) variability by comparing chemical stratigraphies, *Microchem. J.*, 92, 7-14,
881 doi:10.1016/j.microc.2008.08.007, 2009.

882 Traversi, R., Udisti, R., Frosini, D., Becagli, S., Ciardini, V., Funke, B., Lanconelli, C., Petkov, B., Scarchilli,

883 C., and Severi, M.: Insights on nitrate sources at Dome C (East Antarctic Plateau) from multi-year
884 aerosol and snow records, *Tellus B*, 66, 22550, doi:10.3402/tellusb.v66.22550, 2014.

885 Traversi, R., Usoskin, I., Solanki, S., Becagli, S., Frezzotti, M., Severi, M., Stenni, B., and Udisti, R.:
886 Nitrate in Polar Ice: A New Tracer of Solar Variability, *Sol. Phys.*, 280, 237-254, 2012.

887 Udisti, R., Becagli, S., Benassai, S., Castellano, E., Fattori, I., Innocenti, M., Migliori, A., and Traversi, R.:
888 Atmospheresnow interaction by a comparison between aerosol and uppermost snow-layers
889 composition at Dome C, East Antarctica, *Ann. Glaciol.*, 39, 53-61, 2004.

890 Wagenbach, D., Ducroz, F., Mulvaney, R., Keck, L., Minikin, A., Legrand, M., Hall, J.S., and Wolff, E.W.:
891 Sea-salt aerosol in coastal Antarctic regions, *J. Geophys. Res.*, 103, 10961-10974, 1998a.

892 Wagenbach, D., Graf, V., Minikin, A., Trefzer, U., Kipfstuhl, J., Oerter, H., and Blindow, N.:
893 Reconnaissance of chemical and isotopic firn properties on top of Berkner Island, Antarctica, *Ann.*
894 *Glaciol.*, 20, 307-312, 1994.

895 Wagenbach, D., Legrand, M., Fischer, H., Pichlmayer, F., and Wolff, E.W.: Atmospheric near-surface
896 nitrate at coastal Antarctic sites, *J. Geophys. Res.*, 103, 11007-11020, 1998b.

897 Warren, S.G., Brandt, R.E., and Grenfell, T.C.: Visible and near-ultraviolet absorption spectrum of ice
898 from transmission of solar radiation into snow, *Appl. Optics*, 45, 5320-5334, 2006.

899 Weller, R., Traufetter, F., Fischer, H., Oerter, H., Piel, C., and Miller, H.: Postdepositional losses of
900 methane sulfonate, nitrate, and chloride at the European Project for Ice Coring in Antarctica
901 deep-drilling site in Dronning Maud Land, Antarctica, *J. Geophys. Res.*, 109, 1-9,
902 doi:10.1029/2003JD004189, 2004.

903 Weller, R., and Wagenbach, D., 2007. Year-round chemical aerosol records in continental Antarctica
904 obtained by automatic samplings.

905 Witherow, R.A., Lyons, W.B., Bertler, N.A., Welch, K.A., Mayewski, P.A., Sneed, S.B., Nysten, T., Handley,
906 M.J., and Fountain, A.: The aeolian flux of calcium, chloride and nitrate to the McMurdo Dry Valleys
907 landscape: evidence from snow pit analysis, *Antarct. Sci.*, 18, 497-505,
908 doi:10.1017/S095410200600054X, 2006.

909 Wolff, E.W., 1995. Nitrate in polar ice, in: Delmas, R.J. (Ed.), in *Ice core studies of global*
910 *biogeochemical cycles*. Springer, New York, pp. 195-224.

911 Wolff, E.W., Barbante, S., Becagle, S., Bigler, M., Boutron, C.F., Castellano, E., de Angelis, M., and
912 Federer, U.: Changes in environment over the last 800,000 years from chemical analysis of the EPICA
913 Dome C ice core, *Quaternary Sci. Rev.*, 29, 285-295, 2010.

914 Wolff, E.W., Bigler, M., Curran, M., Dibb, J., Frey, M., Legrand, M., and McConnell, J.: The Carrington
915 event not observed in most ice core nitrate records, *Geophys. Res. Lett.*, 39, L08503,
916 doi:10.1029/2012GL051603, 2012.

917 Wolff, E.W., Bigler, M., Curran, M.A.J., Dibb, J.E., Frey, M.M., Legrand, M., and McConnell, J.R.:
918 Comment on "Low time resolution analysis of polar ice cores cannot detect impulsive nitrate events"
919 by D.F. Smart et al, *J. Geophys. Res.*, 121, 1920-1924, 2016.

920 Wolff, E.W., Jones, A.E., Bauguitte, S.-B., and Salmon, R.A.: The interpretation of spikes and trends in
921 concentration of nitrate in polar ice cores, based on evidence from snow and atmospheric
922 measurements, *Atmos. Chem. Phys.*, 8, 5627-5634, 2008.

923 Xiao, C., Mayewski, P.A., Qin, D., Li, Z., Zhang, M., and Yan, Y.: Sea level pressure variability over the
924 southern Indian Ocean inferred from a glaciochemical record in Princess Elizabeth Land, east
925 Antarctica, *J. Geophys. Res.*, 109, doi:10.1029/2003JD004065, 2004.

926 Zatkan, M., Grenfell, T., Alexander, B., Doherty, S., Thomas, J., and Yang, X.: The influence of snow grain

927 size and impurities on the vertical profiles of actinic flux and associated NO_x emissions on the
928 Antarctic and Greenland ice sheets, *Atmos. Chem. Phys.*, 13, 3547-3567,
929 doi:10.5194/acp-13-3547-2013, 2013.

930 Zatzko, M.C., Geng, L., Alexander, B., Sofen, E.D., and Klein, K.: The impact of snow nitrate photolysis on
931 boundary layer chemistry and the recycling and redistribution of reactive nitrogen across Antarctica
932 and Greenland in a global chemical transport model, *Atmos. Chem. Phys.*, 16, 2819-2842,
933 doi:10.5194/acp-16-2819-2016, 2016.

934 Zeller, E.J., Dreschhoff, G.A., and Laird, C.M.: Nitrate flux on the Ross Ice Shelf, Antarctica and its
935 relation to solar cosmic rays, *Geophys. Res. Lett.*, 13, 1264-1267, 1986.

936

937

938 **Table 1.** Snowpit information on the traverse from coastal Zhongshan Station to Dome A, East
 939 Antarctica.

Snowpit No.	Latitude, °	Longitude, °	Elevation, m	Distance to coast, km	Annual snow accumulation, $\text{kg m}^{-2} \text{a}^{-1}$)	Depth, cm	Sampling resolution, cm	Sampling year
SP1	-70.52	76.83	1613	132	193.2	150	5.0	2010/2011
SP2	-71.13	77.31	2037	200	172.0	150	3.0	2012/2013
SP3	-71.81	77.89	2295	283	99.4	200	5.0	2012/2013
SP4	-72.73	77.45	2489	387	98.3	200	5.0	2012/2013
SP5	-73.40	77.00	2545	452	90.7	200	5.0	2012/2013
SP6	-73.86	76.98	2627	514	24.6	300	2.5	2012/2013
SP7	-74.50	77.03	2696	585	29.2	100	2.0	2012/2013
SP8	-74.65	77.01	2734	602	80.2	180	2.0	2010/2011
SP9	-76.29	77.03	2843	787	54.8	200	2.0	2012/2013
SP10	-76.54	77.02	2815	810	100.7	240	3.0	2010/2011
SP11	-77.13	76.98	2928	879	81.2	200	2.5	2012/2013
SP12	-77.26	76.96	2962	893	83.4	265	5.0	2009/2010
SP13	-77.91	77.13	3154	968	33.3	200	2.0	2012/2013
SP14	-78.34	77.00	3368	1015	87.6	216	3.0	2010/2011
SP15	-78.35	77.00	3366	1017	70.0	162	2.0	2009/2010
SP16	-79.02	76.98	3738	1092	25.4	200	2.5	2012/2013
SP17	-79.65	77.21	3969	1162	46.2	130	2.0	2010/2011
SP18	-80.40	77.15	4093	1250	24.2	300	2.0	2010/2011
SP19	-80.41	77.11	4092	1254	23.7	300	1.0	2009/2010
SP20	-80.42	77.12	4093	1256	23.5	300	2.5	2012/2013
Core 1 ²⁾	-70.83	77.08	1850	168	127.0	-	-	1996/1997
Core 2 ³⁾	-76.53	77.03	2814	813	101.0	-	-	1998/1999

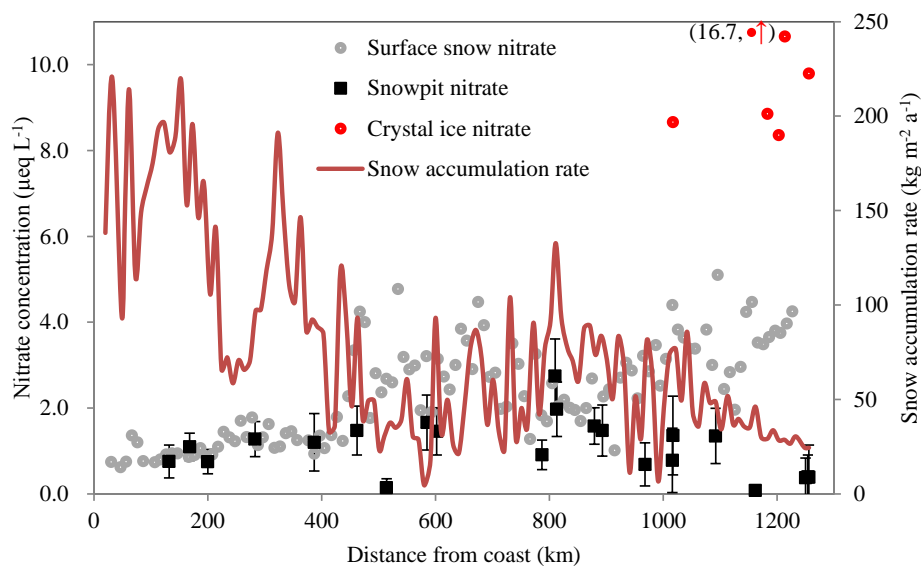
940 1) Annual snow accumulation rate is obtained from the field bamboo stick measurements (2009 - 2013),
 941 updated from the report (Ding et al., 2011). Note that snow accumulation rate at the two ice core sites
 942 are derived from ice core measurements.

943 2) Core 1, ice core data of previous report (Li et al., 1999; Xiao et al., 2004).

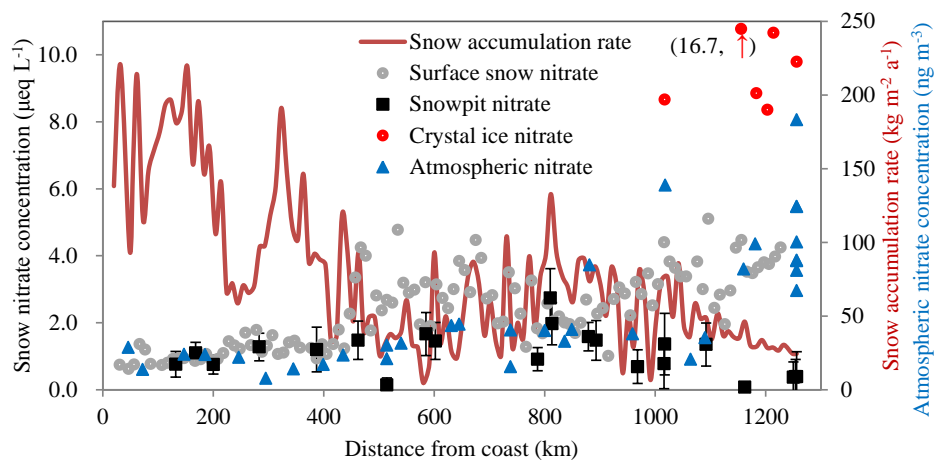
944 3) Core 2, ice core data of previous report (Li et al., 2009).

945

带格式的: 字体颜色: 文字 1



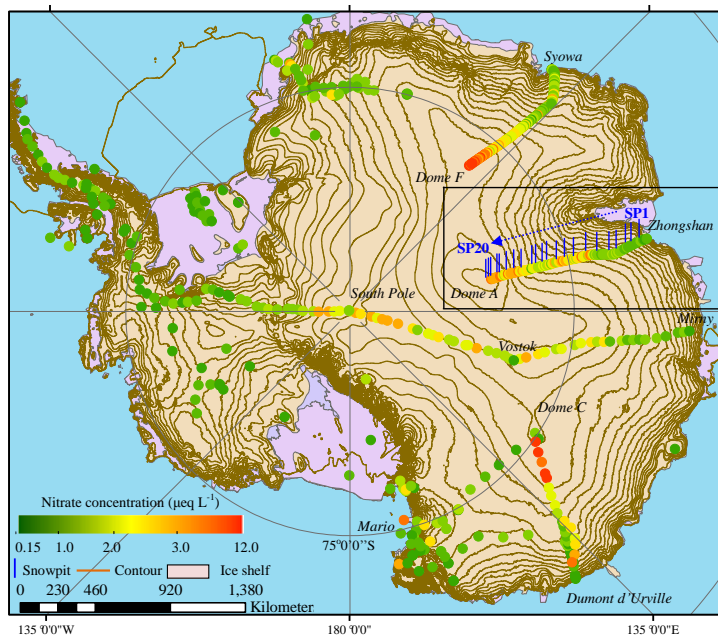
946



947

948 **Figure 1.** Concentrations of NO_3^- in snow (surface snow, crystal ice and snowpits; on the primary
949 y-axis) and atmosphere (on the secondary y-axis), with error bars representing one standard deviation
950 of NO_3^- (1σ) for individual snowpits. Also shown is the annual snow accumulation rate on the traverse
951 (red solid line; based on Ding et al. (2011)). Note that NO_3^- concentration in one crystal ice sample (red
952 dot), 16.7 $\mu\text{eq L}^{-1}$ in the parentheses, is higher than the maximum value of the primary y-axis (NO_3^-
953 concentration = 16.7 $\mu\text{eq L}^{-1}$ in the parentheses).
954

955



956

957

958

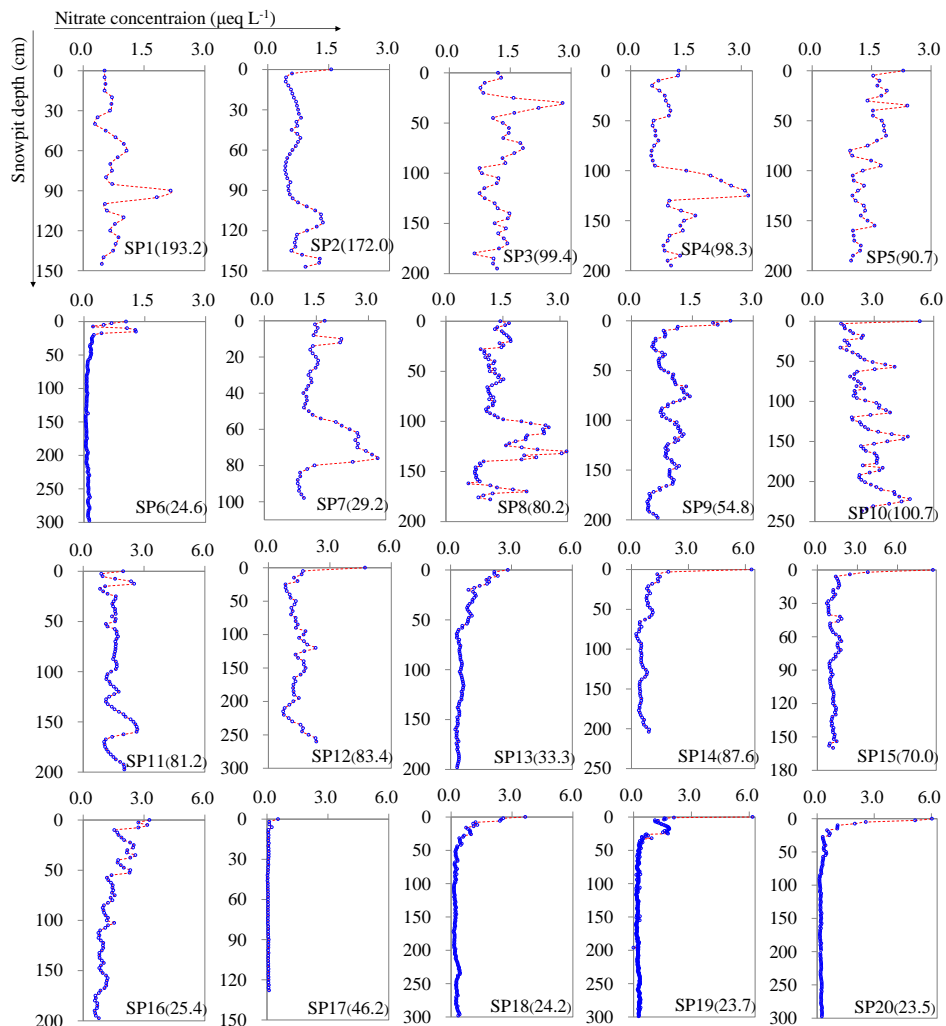
959

960

961

962

Figure 2. Concentrations of NO_3^- in surface snow across Antarctica. Note that the values of crystal ice around Dome A were not included. The data of DDU to Dome C is from Frey et al. (2009). The other surface snow NO_3^- concentrations are from the compiled data (Bertler et al., 2005 and references therein). Also illustrated are the locations of snowpits on the traverse route from Zhongshan to Dome A in this study (SP1 to SP20, solid short blue line; Table 1).



964

965

966

967

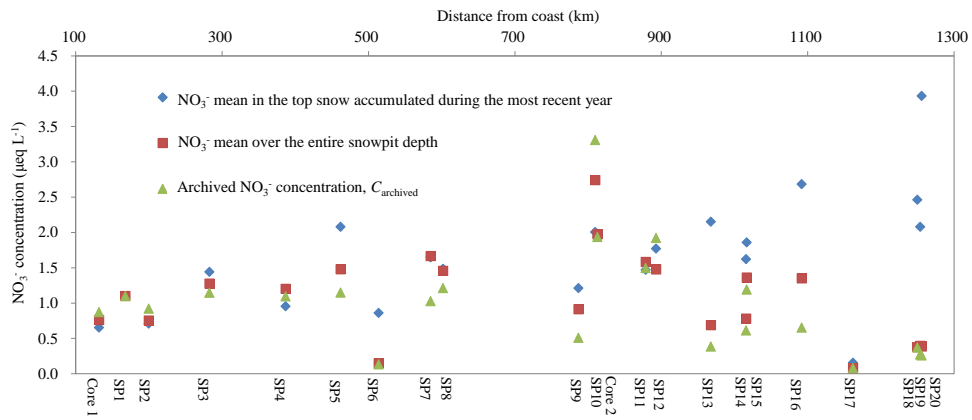
968

969

970

Figure 3. The full profiles of NO_3^- concentrations for snowpits collected on the traverse from the coast to Dome A, East Antarctica (SP1 is closest the coast; SP20 the furthest inland; see Figure 2). The details on sampling of the snowpits refer to Table 1. The numbers in parentheses in each panel denote the annual snow accumulation rates ($\text{kg m}^{-2} \text{a}^{-1}$). Note that the scales of x-axes for the snowpits SP1 – SP9 and SP10 – SP-20 are different.

971



972

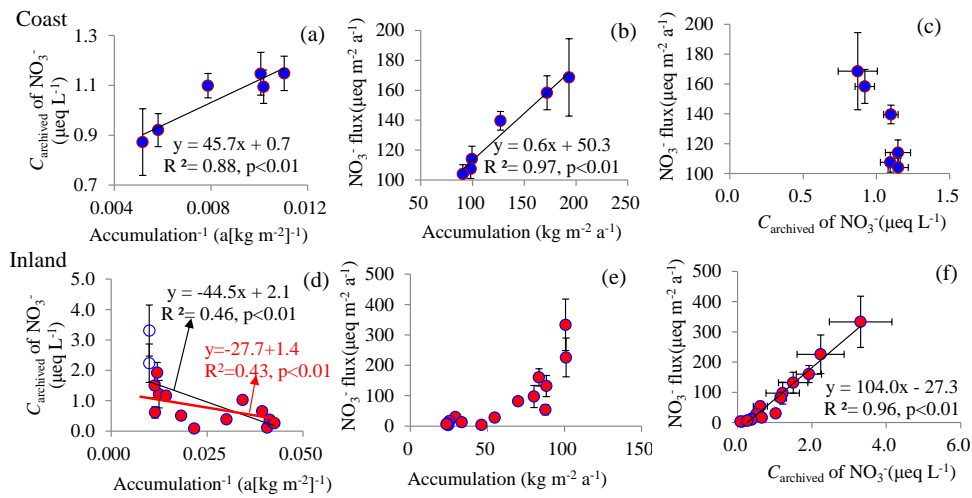
973

974

975

976

Figure 4. Mean concentrations of NO_3^- for the entire snowpit depth (in square), the uppermost layer covering one-year snow accumulation (in diamond) and the bottom layer covering a full annual cycle of deposition (archived NO_3^- concentration, C_{archived} , in triangle).

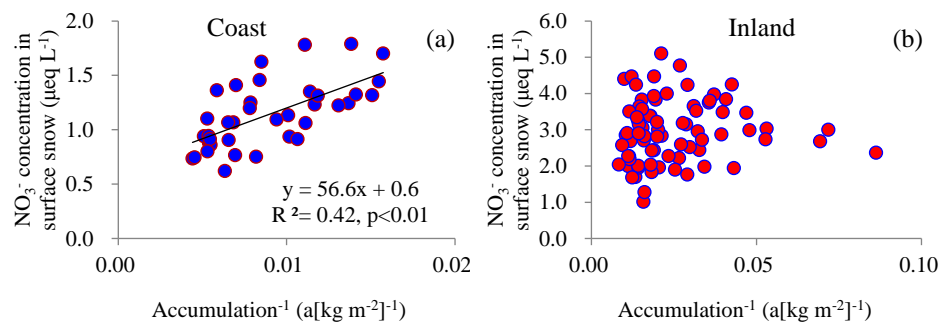


978

979

Figure 5. The relationships among st snow accumulation rate, the archived concentration (C_{archived}), and
 980 flux of NO_3^- in coastal (top row, (a), (b) and (c)) and inland (bottom row, (d), (e) and (f)) Antarctica. In
 981 panel (d), the linear fit in black line ($y = -44.5x + 2.1$) includes the full date-data set, while the linear
 982 equation in red ($y = -27.7x + 1.5$) was obtained by excluding two cases (open circles) with snow
 983 accumulation rate larger than $100 \text{ kg m}^{-2} \text{ a}^{-1}$ (see the main text). The flux values are the product of
 984 C_{archived} of NO_3^- and snow accumulation rate, namely the archived flux. Least squares regressions are
 985 noted with solid lines and are significant at $p < 0.01$. Error bars represent one standard deviation (1σ).
 986

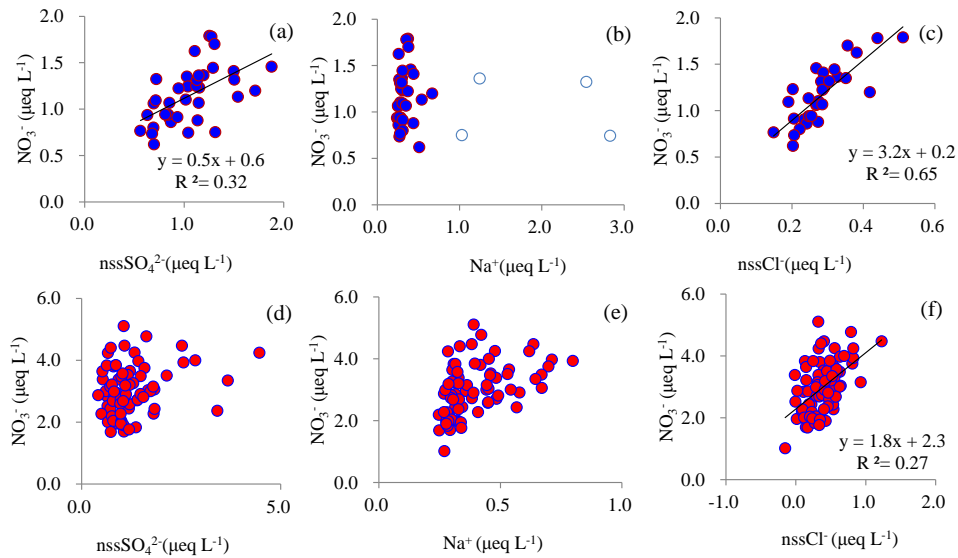
987
988



989
990
991
992
993

Figure 6. The relationships between NO_3^- concentration and inverse snow accumulation rate in surface snow in coastal (panel (a)) and inland (panel (b)) Antarctica. Least squares regressions are noted with solid line and are significant at $p < 0.01$.

994



995

996

997

998

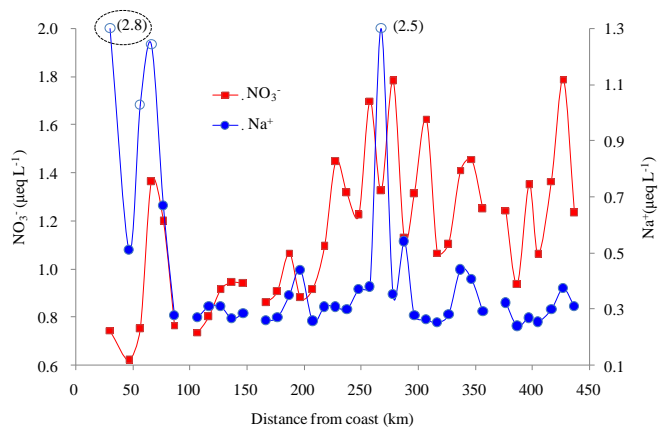
999

1000

1001

Figure 7. Relationships between NO_3^- and co-existing major ions in surface snow in coastal (top row, (a), (b) and (c)) and inland (bottom row, (d), (e) and (f)) Antarctica. Least squares regressions are noted with solid line and are significant at $p < 0.01$. The 4 samples with high Na^+ concentrations are denoted by blue open circles (b), the same as those in Figure 8 (the blue open circles). Note that the 4 samples were excluded in the plot of NO_3^- vs. nssCl^- (c).

1002



1003

1004

1005

1006

1007

1008

1009

Figure 8. Concentrations of NO_3^- and Na^+ in surface snow samples on the coast. Four samples with high Na^+ concentrations are denoted by open circles, corresponding to those in Fig. 7b. Note that Na^+ concentrations in two samples, 2.5 and 2.8 $\mu\text{eq L}^{-1}$ in parentheses, are above the maximum value of the secondary y-axis (Na^+ concentration). The sample in the dashed ellipse, with Na^+ concentration of 2.8 $\mu\text{eq L}^{-1}$, is the fresh snowfall.